RMetS
Royal Meteorological Society

Atmospheric ions and new particle formation events at a tropical location, Pune, India

A. K. Kamra,[a] Devendraa Siingh,[a]*A. S. Gautam,[a] V. P. Kanawade,[b,c] S. N. Tripathi[b] and A. K. Srivastava[d]

[a]*Indian Institute of Tropical Meteorology, Pune, India*
[b]*Department of Civil Engineering, Centre for Environmental Engineering, Indian Institute of Technology Kanpur, India*
[c]*Department of Physical Geography and Ecosystem Science, Lund University, Sweden*
[d]*Indian Institute of Tropical Meteorology (Branch), New Delhi, India*

*Correspondence to: Devendraa Siingh, Indian Institute of Tropical Meteorology, Dr Homi Bhabha Road, Pashan, Pune 411 008, India. E-mail: devendraasiingh@tropmet.res.in; devendraasiingh@gmail.com

Characteristics of small, intermediate and large ions and nanometre particles, and the influences of environmental conditions and local topography on the interactions of these ions and particles in the size range of 3.85–47.8 nm diameter are studied during new particle formation (NPF) events observed at Pune, India from 20 March to 23 May 2012. During the NPF events, the formation rate of 5 nm particles ranged from 3.5 to 13.9 cm^{-3} $s^{-1}$and growth rates of both positive and negative ions were greater than those of neutral particles. Total ion concentrations in this size range were approximately double on event days than on non-event days. The NPF events were generally preceded by 2–3 h periods of enhanced concentration of ions and aerosols (PECIA) which are associated with katabatic winds from the surrounding hill-slopes at our site. During PECIA, ions $\leq$8 nm diameter grew faster and attained mode diameters greater than those of neutral particles. PECIA provided the ions of sub-8 nm diameter and dramatically reduced the condensation sinks and thus contributed to the development of conditions conducive for NPF. During PECIA, total concentrations of the ions and particles become almost equal and the Boltzmann charge distribution breaks down. During NPF events, mode diameters of the ions and particles first steeply decreased accompanied by a steep increase in condensation sink but later gradually increased at identical rates.

Observations of charging ratio of 3–4 nm particles being higher than the charge equilibrium value and non-observation of charge equilibrium for $>$5 nm ions and particles indicate occurrence of ion nucleation and/or advection during the PECIA.

Key Words: new particle formation; ion nucleation; ions; aerosols

Received 9 December 2014; Revised 12 May 2015; Accepted 2 June 2015; Published online in Wiley Online Library 12 August 2015

1. Introduction

Terrestrial radioactivity and cosmic rays are the main sources of ionization in the troposphere on a global scale (Hoppel *et al.*, *1986*). The ionization produced by radioactive radiation from the ground and the radioactive gases and their daughter products such as radon (^{220}Ra and ^{222}Ra) exhaled from the ground generally dominates in the lowest 1 km of the atmospheric boundary layer over the land surface. On the other hand, cosmic rays generate primary ions deep within the troposphere and are the main source of small ion production above ~1 km from the ground (Hoppel *et al.*, 1986). In addition to these two main sources which add equal numbers of small ions of each polarity, some other processes such as dust storms, combustion, raindrops splashing on the Earth's surface, breaking ocean waves, corona discharge occurring at sharp points and tree branches below thunderstorms, waterfalls and volcanoes all introduce a net charge into the atmosphere (Blanchard, 1963; Anderson, 1965; Kamra, 1969, 1972a, 1972b, 1989; Gopalakrishnan *et al.*, 1996, 2005; Yu, 2001; Laakso *et al.*, 2007; Luts *et al.*, 2009; Kolarz *et al.*, 2012).

In recent years, the studies of ions have received additional impetus because atmospheric ions have been proposed as significantly contributing to the nucleation and growth processes of particles (Yu and Turco, 2000, 2011; Lee *et al.*, 2003; Lovejoy *et al.*, 2004; Kanawade and Tripathi, 2006; Siingh *et al.*, 2011). The entire mobility distribution of the atmospheric ions can be

divided in two main classes: (i) cluster ions (mobility $\geq$0.5 $cm^2 V^{-1} s^{-1}$, diameter $\leq$1.6 nm) and (ii) aerosol ions (charged aerosol particles, mobility <0.5 $cm^2V^{-1}s^{-1}$, diameter >1.6 nm) (Hõrrak *et al.*, 2003). These two classes can be divided into five independent air ion categories i.e. small cluster ions (mobility 3.2–1.3 $cm^2V^{-1}s^{-1}$, size 0.46–0.85 nm diameter), big cluster ions (mobility 1.3–0.5 $cm^2V^{-1}s^{-1}$, size 0.85–1.6 nm diameter), intermediate ions (0.5–0.034 $cm^2V^{-1}s^{-1}$, size 1.6–7.4 nm diameter), light large ions (mobility 0.034–0.0042 $cm^2V^{-1}s^{-1}$, size 7.4–22 nm diameter), and heavy large ions (mobility 0.0042–0.00087 $cm^2V^{-1}s^{-1}$, 22–79 nm diameter) (Hõrrak *et al.*, 2003). Particle formation in the intermediate size range gains further importance in view of the recent study of Tammet *et al.* (2013) that formation of such particles also occurs during the quiet periods between events of intensive nucleation of atmospheric particles. Also, charge on newly formed particles can significantly change the aerosol coagulation and scavenging characteristics (Tinsley *et al.*, 2000; Tripathi and Harrison, 2002; Rawal *et al.*, 2013).

High particle concentrations observed in the clean marine boundary layer and clean continental sites cannot be explained by the homogeneous binary nucleation process alone (Covert *et al.*, 1996; Weber *et al.*, 1997). Several processes such as homogeneous ternary nucleation (Kulmala *et al.*, 2000, 2013; Merikanto *et al.*, 2007), ion nucleation clusters (Lee *et al.*, 2003; Lovejoy *et al.*, 2004; Eisele *et al.*, 2006; Kanawade and Tripathi, 2006; Lida *et al.*, 2006; Yu *et al.*, 2008, 2010; Yli-Juuti *et al.*, 2009; Gagné *et al.*, 2010; Yu and Turco, 2011; Gonser *et al.*, 2014), activation of neutral clusters (e.g. Kulmala *et al.*, 2006) and the effect of organic gases on nucleation (O'Dowd *et al.*, 2002; Zhang *et al.*, 2004; Tunved *et al.*, 2006; Laaksonen *et al.*, 2008; Metzger *et al.*, 2010) have been proposed to explain high rates of particle formation. From their four years of measurements at a mountain observatory, García *et al.* (2014) conclude that SO_2 concentrations in the range of 60–300 ppt seem to be most influencing parameters in the year-to-year variability in the frequency of new particle formation (NPF) events. Recent observations of Kulmala *et al.* (2013) revealed that NPF occurs by forming stable critical clusters (diameter 1.5 $\pm$ 0.3 nm) followed by subsequent growth to 2 and 3 nm. Hõrrak *et al.*'s (1998) observations of bursts of intermediate ions in air support the ion-induced nucleation explanation. Further, simultaneous measurements of ions and aerosol show increase of condensation nuclei associated with increased rate of ionization (Harrison and Aplin, 2001; Hirsikko *et al.*, 2007; Vartiainen *et al.*, 2007; Gonser *et al.*, 2014). Kulmala *et al.* (2000) and Modgil *et al.* (2005) showed that high concentration of ultrafine condensation nuclei in a burst event agreed with their model calculations assuming ion-mediated nucleation of H_2SO_4 - H_2O aerosols. On the contrary, Manninen *et al.* (2009a) observed a minor contribution of ion-induced nucleation in field experiments at Hyytiälä, Finland. Based on ion–aerosol microphysical modelling, Yu and Turco (2000) found that charged molecular clusters can grow significantly faster than neutral clusters to reach the size of condensation nuclei that can become cloud condensation nuclei (>80 nm) under specific atmospheric conditions. Concentration of newly formed ultrafine particles is mainly determined by the rates of new particle formation and scavenging by the large pre-existing background aerosol particles (Harrison and Carslaw, 2003).

Small ions, soon after their production, either recombine with ions of opposite polarity and neutralize each other or attach to the neutral particles. Charge distribution on the particles is normally determined by the Boltzmann distribution (Keefe *et al.*, 1959). If the concentrations and mobilities of ions of opposite polarity are not equal, the Boltzmann distribution of charges breaks down. It can happen under several conditions in the atmosphere. For example, Hussin *et al.* (1983) found in his experiments that Boltzmann charge distribution for nanometre particles is not validated for particles in the size range of 4–30 nm. It is well recognized that Boltzmann charge distribution breaks down for small-size particles of below 100 nm diameter (Hoppel and Frick, 1986). However, the value of the attachment coefficient, used for the calculations, determines the link between mass and mobility of ions and thus the final charge distribution. Further, coagulation of particles leads to a shift in their size distribution to larger particles and reduces the build-up of extremely high concentrations of ultrafine particles produced by the gas-to-particle conversion (Harrison and Carslaw, 2003). Thus, knowledge of ions and the charged fractions of particles during nucleation events could be helpful in understanding the contribution of different nucleation mechanisms.

Recently, NPF events have been reported to occur at nighttime and at high altitude sites (Venzac *et al.*, 2007; Lee *et al.*, 2008; Boulon *et al.*, 2010; Ortega *et al.*, 2012; Gonser *et al.*, 2014; Kecorius *et al.*, 2015). It has been reported that transportation of air masses in valleys and the variations in radon concentration and the ionization produced by it can influence the formation and growth of new particles. We propose to investigate such influences on diurnal cycles of ions and particles at our site which is also located near hills and is described in detail in section 2.5. The present study aims at understanding the formation and growth characteristics of ions and particles and to study the influences of environmental conditions and local topography on their interactions. Since the ions can lower the critical stable size of the clusters that can grow to cloud condensation ion nuclei, an attempt has been made to understand the relative roles of ion nucleation and neutral cluster nucleation mechanisms in the formation and growth processes of ions and particles during NPF events.

In this article, we present simultaneous measurements of number size distributions of ions and aerosol particles in the size ranges of 0.46–47.8 nm diameter and 3.85–135.8 nm diameter, respectively, during 20 March 2012 to 23 May 2012 at an urban site, Pune, in the tropical Indian subcontinent. The rates of formation and growth of positive/negative ions and particles have been calculated. From our simultaneous measurements of ions and particles in the common size range of 3.85–47.8 nm the influences of the local topography and environmental conditions on ion–particle interactions have been studied during the NPF events. Since radon and its daughter products dominate in the formation of primary ions close to the land surface and these ions have been proposed to significantly contribute to the nucleation and growth of particles (e.g. Gonser *et al.*, 2014), simultaneous measurements of radon and its progeny have also been made in order to understand the role of ions in the mechanism responsible for the formation and growth of new particles. A comparative study of particle size distributions observed at this site and at Kanpur during the period of 15 April to 23 May is reported by Kanawade *et al.* (2014).

2. Instrumentation and observation site

2.1. Ion measurements

A Neutral cluster and Air Ion Spectrometer (NAIS) measures the ion and particle number size distributions in 28 size bins

simultaneously by running the instrument alternately in the corresponding operating modes with a 1 min (minimum period) resolution to optimize its sensitivity and signal-to-noise ratio. However, NAIS was operated only in ion mode in the present study. NAIS uses two unipolar corona dischargers to charge the sampled particles and for their subsequent detection. Basically, it has two identical cylindrical aspiration-type differential mobility analysers (DMA), one for positive ions and the other for negative ions. Naturally charged particles, carried by air flow, drift in the radial electric field and are deposited on different electrodes of the DMA according to their electrical mobilities. Each DMA has 21 insulated collectors and the current carried by ions to each collector is amplified and measured separately. Detailed information about the NAIS and the software can be found on website: http://airel.ee and in Manninen *et al.* (2009b) and Mirme and Mirme (2013). The site location, installation and some preliminary results are given in detail by Siingh *et al.* (2013).

The average mobility for positive and negative ions is obtained over a 5 min period, based on 200 s sample air and 100 s offset-level measurements. We have divided our data into five categories as described by Hõrrak *et al.* (2003). However, in our observations, the upper range of heavy large ions was limited to the mobility range of 0.0042–0.00133 $cm^2\ V^{-1}\ s^{-1}$ (size 22–47.8 nm diameter). Here, we have used the procedure of Tammet (1995) and Hõrrak *et al.* (2003) for the mobility-to-diameter conversion. The first two and the last two of Hõrrak *et al.*'s (2003) categories can be merged with each other to describe results in three categories, i.e. cluster, intermediate and large ions. However, we prefer here to present our results with higher size-dependent categorization in order to learn more of ion-growth processes which are highly size dependent.

2.2. *Aerosol particle measurements*

Particle size distributions were measured using a scanning mobility particle sizer (SMPS) in the diameter range of 13–750 nm using a long-differential mobility analyser (LDMA, TSI 3081) in combination with a butanol condensation particle counter (CPC, TSI 3775) from 20 March to 15 April 2012 and in the size range of 3.85–135.8 nm with a nano-differential mobility analyser (NDMA, TSI 3085) in combination with the same butanol CPC from 16 April to 23 May 2012. More details can be found elsewhere (Kanawade *et al.*, 2014).

2.3. *Radon measurements*

Radon and its progeny gas concentrations were simultaneously measured using an RTM 2200 radon detector of SARAD Gmbh, Germany (http://www.sarad.de/). Details of this technique are given in section 3.1.

2.4. *Measurements of meteorological parameters*

Meteorological parameters such as temperature, relative humidity, wind speed, wind direction and solar radiation were obtained from the India Meteorological Department (IMD) observatory at Pune (located about 200 m away from our sampling site). Air temperature and relative humidity were measured using Sutron Corporation (USA) thermistor- and capacitive-type sensors, with an accuracy of ±0.2° C and ±3%, and resolution of 0.1° C and 1%, respectively. Wind speed and direction were measured using Gill Instruments (UK) ultrasonic-type sensors, with an accuracy of 1.2 m s^{-1} and 1°, and resolution of 0.1 m s^{-1} and 1°, respectively. A LI-COR (USA) silicon photodiode-type pyranometer LI-200SZ

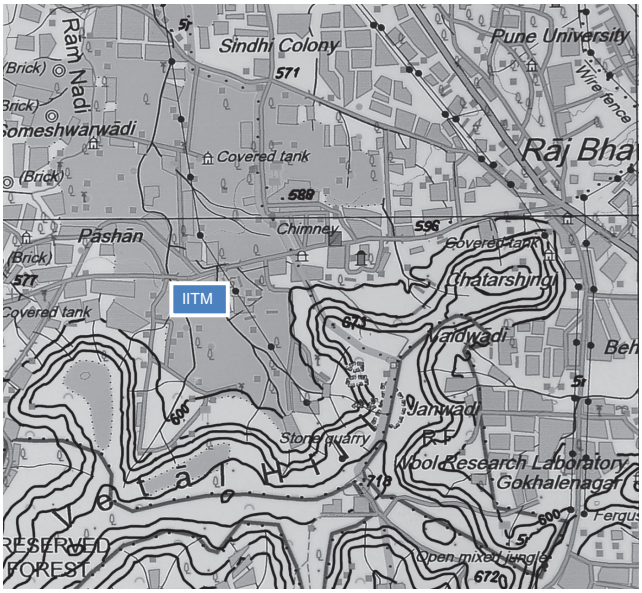

Figure 1. Topography and surroundings of the land around the measurement site at Indian Institute of Tropical Meteorology campus, Pune (India). Numbers on contours correspond to the altitude (m) above mean sea level, 'Covered tank' are the covered water tanks, and 'Chimney' does not exist at present.

Figure 2. Photograph of inlet for NAIS.

is used for measurement of global solar radiation in the wavelength range of 0.3–4 μm, with an accuracy of 5% (Ranalkar *et al.*, 2012).

2.5. *Observation site*

The NAIS, SMPS and RTM 2200 were placed inside a laboratory on the second floor of a three-storey building of the Indian Institute of Tropical Meteorology, Pune (18°31′N, 73°55′E, 560 m above mean sea level), India. The institute is located on the outskirts of a moderately big city with a population of over ∼9 million and population density of 603 km^{-2}as per the 2011 census report. The institute building is surrounded by 500–800 m high hills in the northeast, south and west directions (Figure 1). Hills are closest and very steep to the southeast of the measuring site. An 8 m wide road with moderate traffic runs in the east–west direction about 100 m away from the institute building. A small canteen and a residential area are about 200 and 400 m away, respectively, from the sampling site. However, these sources of pollution had no apparent influences on our measurements. The area is covered with cotton soil. The inlet for NAIS consisted of a metallic pipe of 40 cm length and 3 cm diameter. To minimize the particle loss, the pipe had no sharp turns and was fixed in a cutout (2 × 7 m^2) of the building with its open end facing down at a height of ∼6 m above ground level (Figure 2). The inlet pipe

was shielded from the atmospheric electric field by walls of the building on three sides and a projected roof on the top, but still was well-ventilated to the ambient air.

3. Observations

A 64-day observation campaign by the Indian Institute of Tropical Meteorology, Pune and the Indian Institute of Technology Kanpur, Kanpur (hereafter referred to as IITM-IITK campaign) was carried out at Pune from 20 March to 23 May 2012 to study the characteristics of the NPF events at Pune. During this campaign period, continuous measurements of ions, aerosol particles, radon and meteorological parameters were made. In the following sections, the characteristics of nine NPF events of the type to be described in section 3.2 are discussed. Rates of formation and growth of the ions of both polarities and particles and condensation sinks are calculated for all the nine events observed during our campaign period. However, to illustrate the variability of ions, particles and other parameters and to learn the behavior of ion–particle interactions in this study, we restrict our discussions to a typical NPF event observed on 2 May 2012 and compare the results with those observed on a typical non-event day of 4 May 2012 at this site. The results observed on other event days are qualitatively similar to those observed on 2 May 2012.

3.1. *Environmental factors*

Five-day air-mass back-trajectories using the HYbrid Single-Particle Lagrangian Integrated Trajectory (HYSPLIT) transport and dispersion model (Draxler and Rolph, 2010) calculated for 2 May 2012 show that the air mass reaching the measuring site at 500 m height originated at ∼2000 m level over Iran, travelled southeast to Pakistan and descended to ∼1500–1000 m level before crossing over to the north Arabian Sea where it further descended to ∼500 m level before curling to Mumbai city and arriving over Pune. On the contrary, on 4 May 2012 the air mass originated and travelled from the west at almost sea level and reached Pune without much vertical displacement (Figure 3). On 2 May 2012 surface temperature and relative humidity varied in the range of 20–36.5° C and 17–64%, respectively, and southeasterly winds prevailed at a speed of 0.7–9.0 m s^{-1} at the measuring site (Figure 4). Comparatively, on 4 May 2012, atmospheric temperature remained lower by ∼3° C and relative humidity remained higher by ∼20% for most of the day. Winds were stronger and south-southeasterly in direction, especially in the evening hours, on the non-event day as compared to the event day. Solar irradiance was maximum during noontime and a little higher on 2 May than on 4 May 2012 (Figure 4). Atmospheric pressure was consistently higher by 1–4 mb on 2 May than on 4 May 2012.

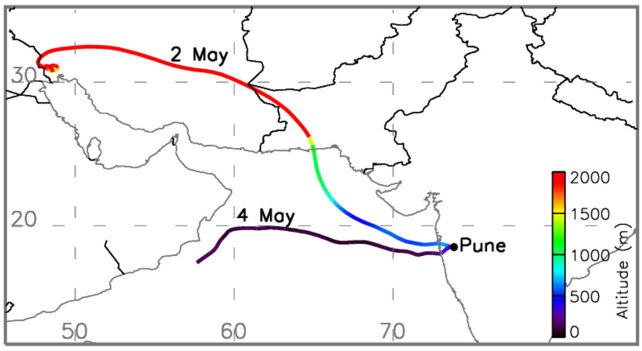

Figure 3. The 5-day NOAA HYSPLIT model back-trajectories of the air masses arriving at 500 m level (Draxler and Rolph, 2010) at the measurement site on 2 and 4 May 2012.

Ionization rate was calculated from measurements of radon by RTM 2200 which provides the equivalent equilibrium concentrations of radon and its progeny, i.e. Po^{218}, Po^{214} and Bi^{214}. As these charged particles traverse through the air, they lose their kinetic energy by collisional and radiative energy losses. Collisional loss includes the energy losses in the excitation and ionization of the atom. Ionization creates ion-pairs and the ion production rate due to radon and its progeny is calculated from

$$q = \varepsilon / I, \tag{1}$$

where

$$\varepsilon = 5.49 \times 10^6 \mathrm{Rn} + 6 \times 10^6 (\mathrm{Po}^{218}) + 7.68 \times 10^6 (\mathrm{Po}^{214}) + 0.85 \times 10^6 (\mathrm{Bi}^{214}) (\text{in Bq m}^{-3}), \tag{2}$$

and where Rn is concentration of radon, Po^{218}, Po^{214} and Bi^{214} are the concentrations of radon progeny (in Bq m^{-3}), ε is total energy (in eV) released by the decay of radon, I is the energy required to produce one ion pair (32 eV) and q is ionization rate (Prasad *et al.*, 2005).

This method, however, does not include the ionization produced by cosmic rays which is about 1–2 ion pairs cm^{-3} s^{-1}(Hoppel *et al.*, 1986; Siingh and Singh, 2010). The values of ionization rate shown in Figure 5 are thus less by this amount. Earlier measurements conducted close to this site also produced comparative values (Kamsali *et al.*, 2011).

3.2. *New particle formation events in ion measurements*

We identified a total of nine NPF events which mostly occurred in the morning between 0830 and 1200 LT (local time, UTC + 5 h 30 min) at our site. In these NPF events a distinct new mode of 4–6 nm appeared in the size range of intermediate ions. The appearance of these particles and their growth towards larger sizes continued for several hours. The shape of the concentration versus time plots in these events resembled a banana shape. However, these were characteristically different from the traditional banana-type events (Laakso *et al.*, 2008; Vana *et al.*, 2008; Lehtipalo *et al.*, 2010; Manninen *et al.*, 2010) observed at other locations, in the respect that they showed neither any burst of small ions nor any persistent growth of ions of <4–6 nm diameter which are typical features of banana-type NPF events. However, these NPF events followed a banana shape for the ion growth from 4–6 to 47.8 nm diameter. We shall classify such events as 'truncated banana' type events. Days with such events are distinctly different from the non-event days when no particle growth is detected. Mobility distributions on non-event days show a deep depression between the cluster ion and large ion modes with very low concentrations of intermediate ions. The traditional banana-type events are typically observed when NPF occurs over a large spatial scale and indicate regional particle formation and growth (Kulmala *et al.*, 2012). The growth of freshly formed particles during the early stage of NPF is due to condensation of vapour on the existing particle surface (Kulmala *et al.*, 2001), while the total number concentration declines in the later stages of NPF mainly because of their coagulation with large particles (Kerminen *et al.*, 2001; Stolzenburg *et al.*, 2005). Figure 6(a) shows time variation of ion size distributions and concentrations of both positive and negative polarities for a typical type of truncated banana event observed here on 2 May 2012. Growth of particles from 4–6 to 47.8 nm diameter can be observed to start from 0914 LT. The average

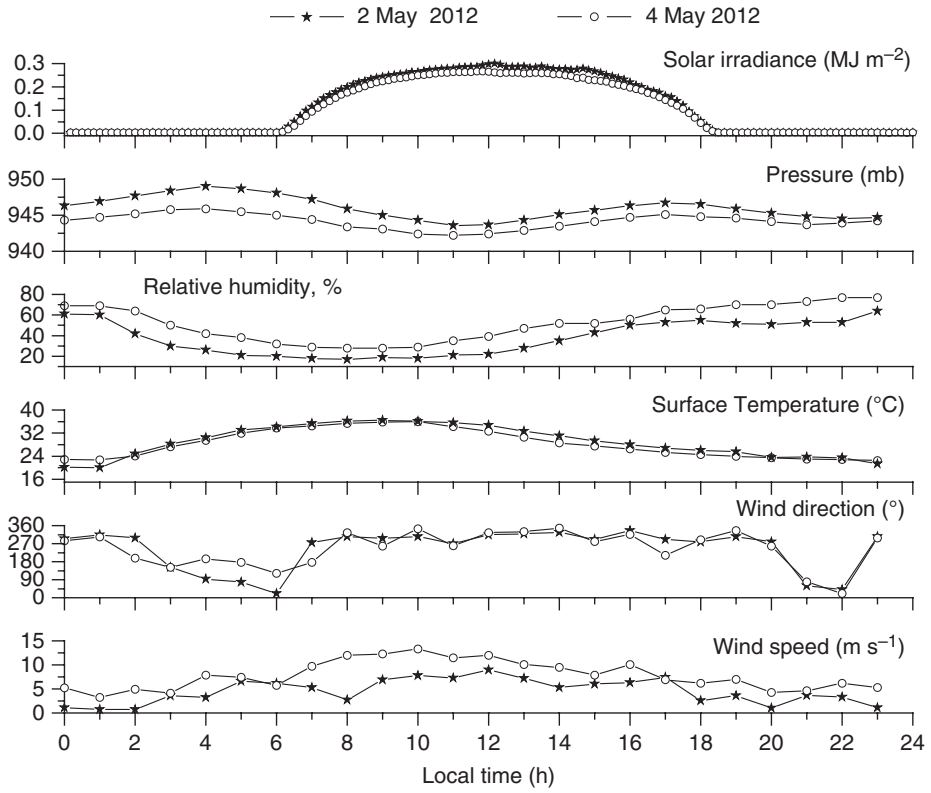

Figure 4. Diurnal variations of meteorological parameters at the measurement site on 2 and 4 May 2012.

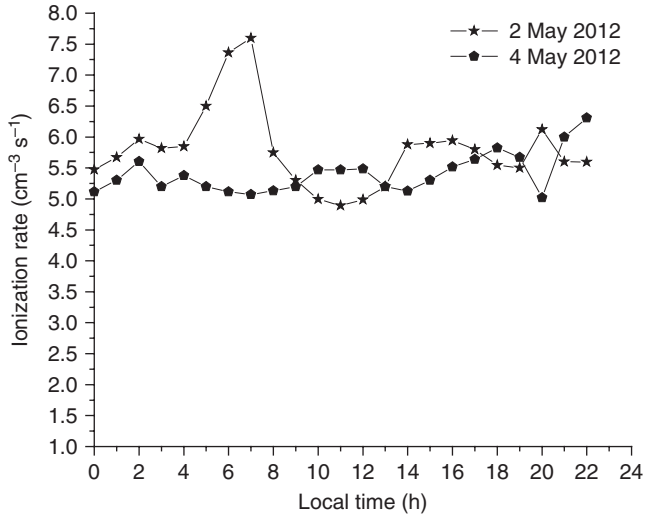

Figure 5. Diurnal variations of the ionization rate (cm^{-3} s^{-1}) calculated from the measurements of radon and its progeny on 2 and 4 May 2012.

growth rates of positive and negative ions, calculated from the method of Shi *et al.* (2007), also followed by Kulmala *et al.* (2004), separately for size ranges of 3.9–25.3 and 25.3–47.8 nm diameters, in this and other events of this type, are shown in the second and third columns of Table 1. In this method, mean diameters are obtained by manually examining each size distribution to identify the particle size that separated freshly nucleated particles from pre-existing particles. Then the number mean diameter values for each of the size ranges are calculated from an average growth rate using the slope of the fitted line joining number mean diameter vs. time.

In all the nine NPF events, growth rates of 3.9–25.3 nm positive (negative) ions are on the average ∼49–142% (49–126%) greater than those of 25.3–47.8 nm positive (negative) ions. Moreover, growth rate of negative ions is always greater (except during one event) than that of positive ions. Our values of ion growth rates given in Table 1 agree well with those of Siingh *et al.* (2013) obtained at the same site during April–May 2010. Moreover, since the growth rates have been observed to be size-dependent, growth rates of 1.9, 3.6 and 4.2 nm h^{-1} observed by Manninen *et al.* (2009a) and Yli-Juuti *et al.* (2011) at Hyytiälä, Finland for all particles in size ranges of 1–3, 3–7 and 7–21 nm, respectively, are less than half of the average growth rates observed for nucleation mode particles in our observations at this tropical site. However, the rates of formation and growth of particles observed during the NPF events at this site are much higher than those observed in the higher altitude observations in the Himalayas (Venzac *et al.*, 2008; Neitola *et al.*, 2011) but are comparable to those observed at other urban sites, e.g. at East St Louis (Shi *et al.*, 2007) and at Mexico City (Dunn *et al.*, 2004).

Figure 6(b) shows time evolution of the ion size distributions and concentrations observed for a typical non-event day, 4 May 2012. Average values of total ion concentrations on 2 May, especially during daytime, were approximately double those on 4 May. Moreover, ion concentrations of each polarity on 2 May exhibited a maximum in the early morning between 0500 and 0800 LT. Thereafter, with the appearance of the NPF event on 2 May, total ion concentration kept increasing for the next 3–4 h and maintained those high values for the whole day. Figure 6(a,b) (lower panels) also show the variations of the concentration of small cluster ions, big cluster ions, intermediate ions, light large ions and heavy large ions with local time on the event and non-event days. Occurrence of higher concentrations of the small and big cluster ions of positive polarity throughout the day on both days indicates the manifestation of electrode effect near the Earth's surface (Chalmers, 1967) or the difference in mobilities of positive and negative ions. Extremely low concentrations of small ions in our observations may be due to the fact that the inlet for NAIS is located ∼8 m above the ground surface. It is noticeable in this respect that small ion concentrations at 1 m height in an observatory only about 100 m away from this site were found to be about an order of magnitude higher than in the present measurements (Dhanorkar and Kamra, 1993).

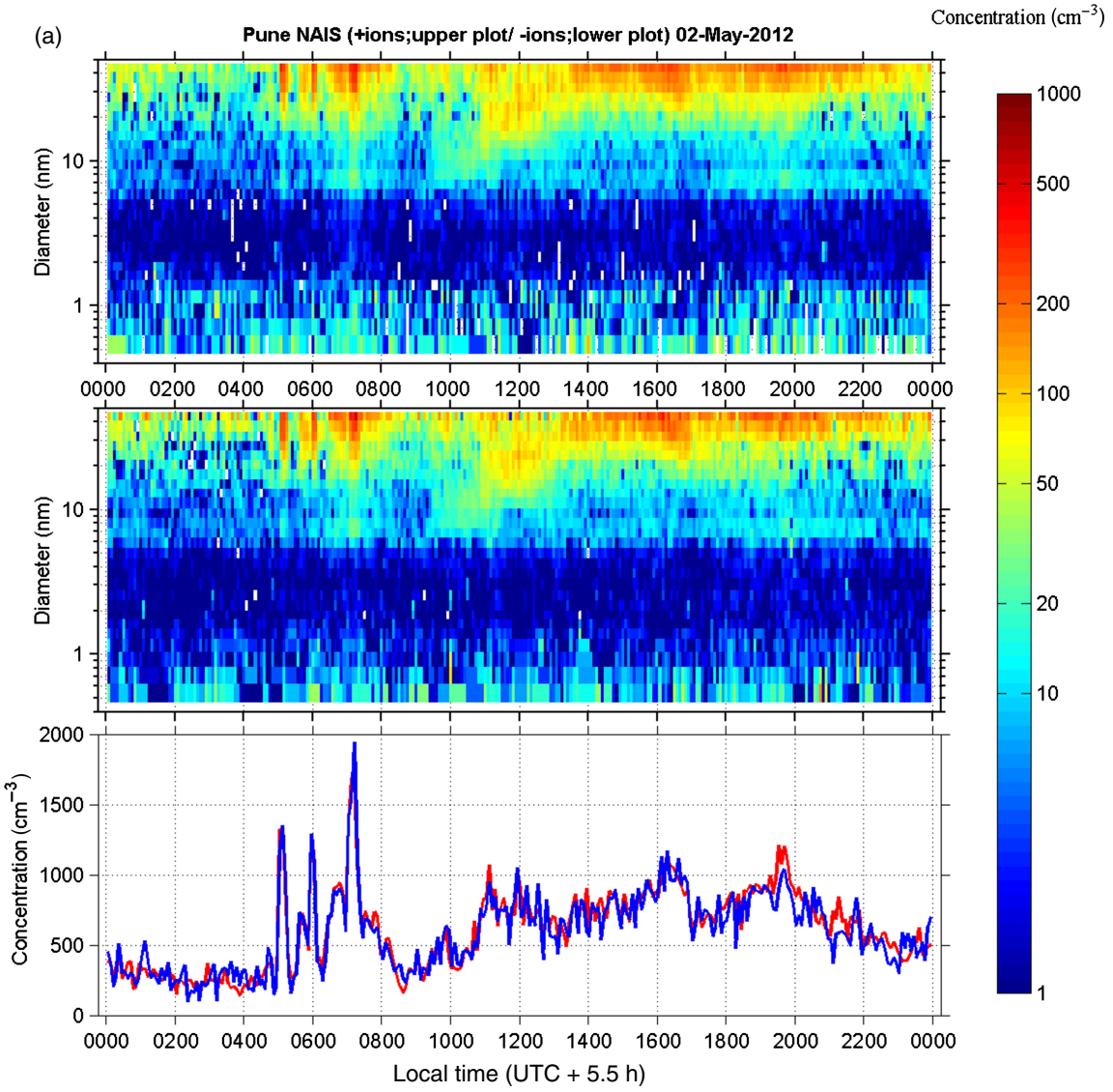

Figure 6. (a) Diurnal variations of ion mobility spectra of positive and negative ions (upper two panels), and concentration of atmospheric ions of both polarities (red line – positive ions, blue line- negative ions) (third panel and, for hourly averages, lower six panels for different categories) on 2 May 2012. (b) As in (a) for 4 May 2012.

3.3. *New particle formation events in aerosol measurements*

Our aerosol particle measurements simultaneously made with SMPS using NDMAS on 2 and 4 May 2012 also exhibited a truncated banana-type NPF event on 2 May 2010 when particles of 3.85 nm diameter grew to a size of >60 nm diameter (Figure 7). The growth of particles continued for the whole day and the calculated average growth rate of particles based on the method of Shi *et al.* (2007) ranged from 5.2 ± 1.9 nm to 9.8 ± 3.9 nm h^{-1} for 3.85–25 nm diameter and from 2.8 ± 0.9 to 6.6 ± 2.2 for 25–47.8 nm diameter particles. The growth rates of positive (negative) ions are 6.2–25.4% (9.5–23.4%) higher than those of particles of corresponding sizes in the size range of 3.9–25.3 nm diameter, and 10.7–60.6% (6.8–72.7%) higher than those of particles in the size range of 25.3–47.8 nm diameter. Moreover, the growth rate of particles observed at this site are comparable to those observed at other urban sites e.g. at Atlanta (McMurry *et al.*, 2005), at Pittsburgh (Stanier *et al.*, 2004), at Beijing (Yue *et al.*, 2009), at Pune (Siingh *et al.*, 2013) and at Kanpur (Kanawade *et al.*, 2014).

The rate of formation of 5 nm particles (J_5) calculated from the method of Dal Maso *et al.* (2005) for different events lies in the range of 3.5–13.9 cm^{-3}s^{-1} (Table 1). These values of J_5 are averages for the period of the event and do not account for the mixing of the air mass being sampled, and therefore may be in error determined by the air mass inhomogeneities in ions, aerosols and condensing vapours. The kinetic model of Yu (2010) for an ion-mediated nucleation mechanism shows that the nucleation rate nonlinearly depends on parameters such as sulphuric acid vapour concentration, temperature, relative humidity, ionization rate and surface area of pre-existing particles which may show large variability from day to day. Moreover, as concluded by Korhonen *et al.* (2011) various tools used to calculate different parameters for NPF events are useful for getting order-of-magnitude estimates of the parameter related to atmospheric nucleation. From this view the value of J_5 needs to be taken as a rough estimate. However, the values of J_5 observed at our site are comparable to those observed at other urban sites at Gual Pahari, India (Mönkkönen *et al.*, 2005), Singapore (Betha *et al.*, 2013) and Beijing (Yue *et al.*, 2009). Table 2 shows the calculated values of condensation sink based on the method of Kulmala *et al.* (2001) at the time of start of the NPF event (CS_{start}) which generally occurs around 0900 LT and as averaged over the NPF time duration (0900–1600 LT) of the event (CS_{avg}). Since low values of condensation sink favour particle formation (Kulmala *et al.*, 2005) it is notable that all values (except in two cases) of CS_{start} are lower than the corresponding CS_{avg} values. However, such a conclusion should not be generalized, especially

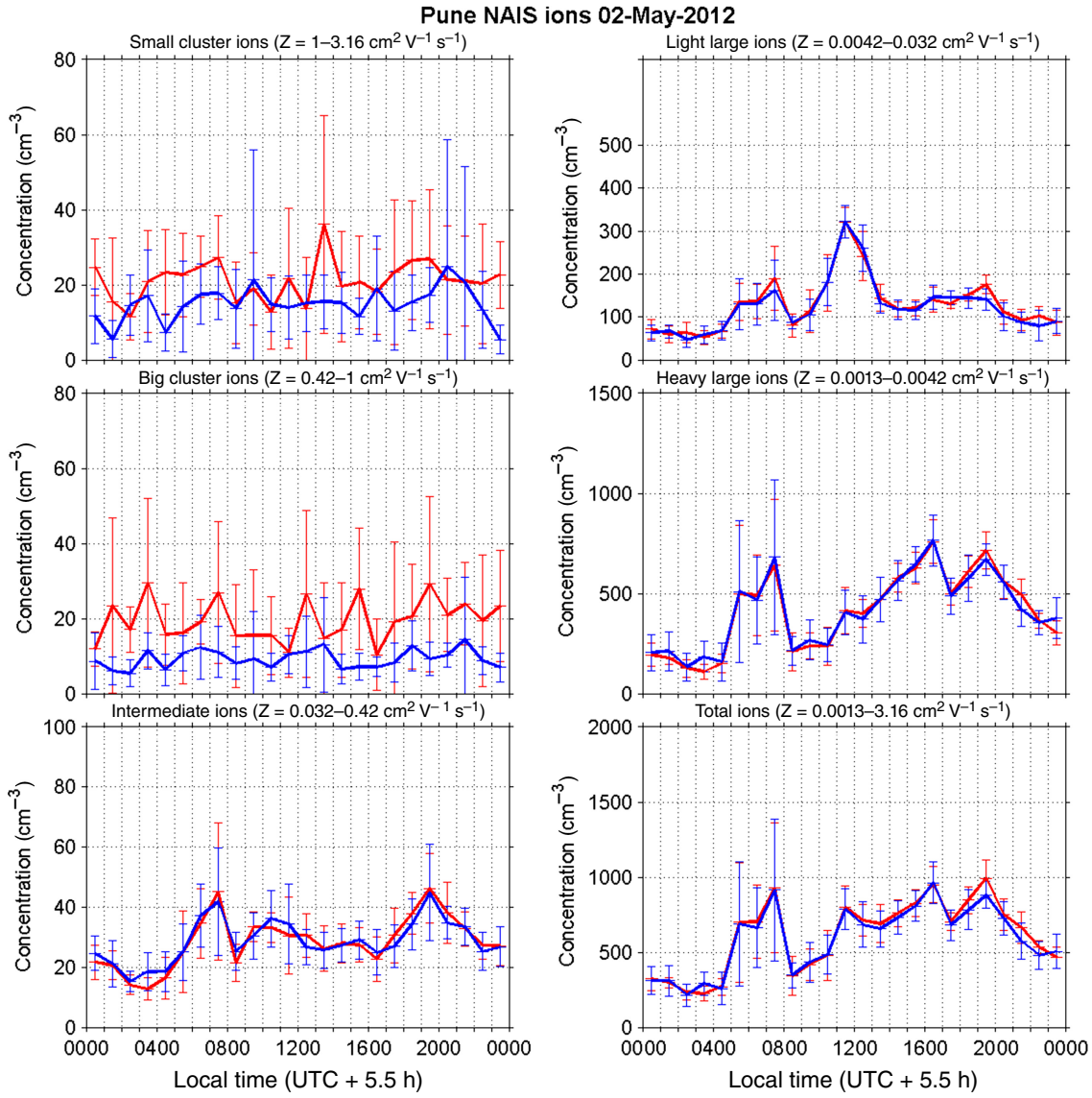

Figure 6. Continued.

for comparison on different days (e.g. on 23 April and 2 May in our observations), since the effect of some other variables such as concentration of condensable vapours dominate the NPF processes on different days (e.g. Yu and Turco, 2011; Kanawade *et al.*, 2014).

3.4. *Period of enhanced concentrations of ions and aerosols*

The NPF events were generally preceded by a 2–3 h period of enhanced concentrations of ions and aerosols (PECIA) that generally occurred between 0600 and 0800 LT (e.g. Figures 6(a,b) and 7). The times of start of NPF events are given in Table 1. Although PECIA occurred most frequently in the early morning hours, it also occurred occasionally at other times, mostly around 2000 LT. During these periods ions did not show any distinctive growth pattern such as banana type. Instead, these periods were characterized by the appearance of high concentrations of ions and aerosol particles in the measured ranges within a short period of the order of minutes. These periods can also be readily recognized in the total ion concentrations versus time record plotted in the third row of Figure 6(a). Prominent among these were the enhancement in concentrations of large ions. PECIA could not be associated with local traffic as the periods and timings of ion/aerosol particle concentration maxima generally preceded by 2–3 h the peak traffic hours, which were ∼0900–1100 LT at this location. Earlier observations of enhancement of ions and conductivity (Dhanorkar and Kamra, 1993) and radon concentrations (Kamsali *et al.*, 2011) observed at the Atmospheric Electricity Observatory,∼100 m away from this site, were also reported during the same period. Such enhancements of ions and aerosol particles can be associated with accumulations of ions, aerosols, radioactive decay products and precursor gases below inversion layers at night-time (Porstendörfer, 1994) and their downward transport with the ketabatic winds along the surrounding hill-slopes in the morning. Occurrence of such a transport process is further discussed in detail in section 4. Such periods of high concentration of ultrafine particles with diameters of 4–9 nm have also been observed by Lee *et al.* (2008) in their night-time troposphere and ground-based observations in Tumbarumba (Australia). The occurrence of PECIA was more frequent than that of NPF events but not necessarily followed by an NPF event. During the 64-day campaign period, the PECIA was observed on 27 days in the early morning hours. Although PECIA occurred on both days, 2 May and 4 May, it was much less intense on the non-event day (4 May) than on the event day (2 May).

3.5. *The common size range in the ion and aerosol measurements*

Figure 8(a,b) shows variations of the hourly averaged size distributions of both ions of either polarity and aerosol particles

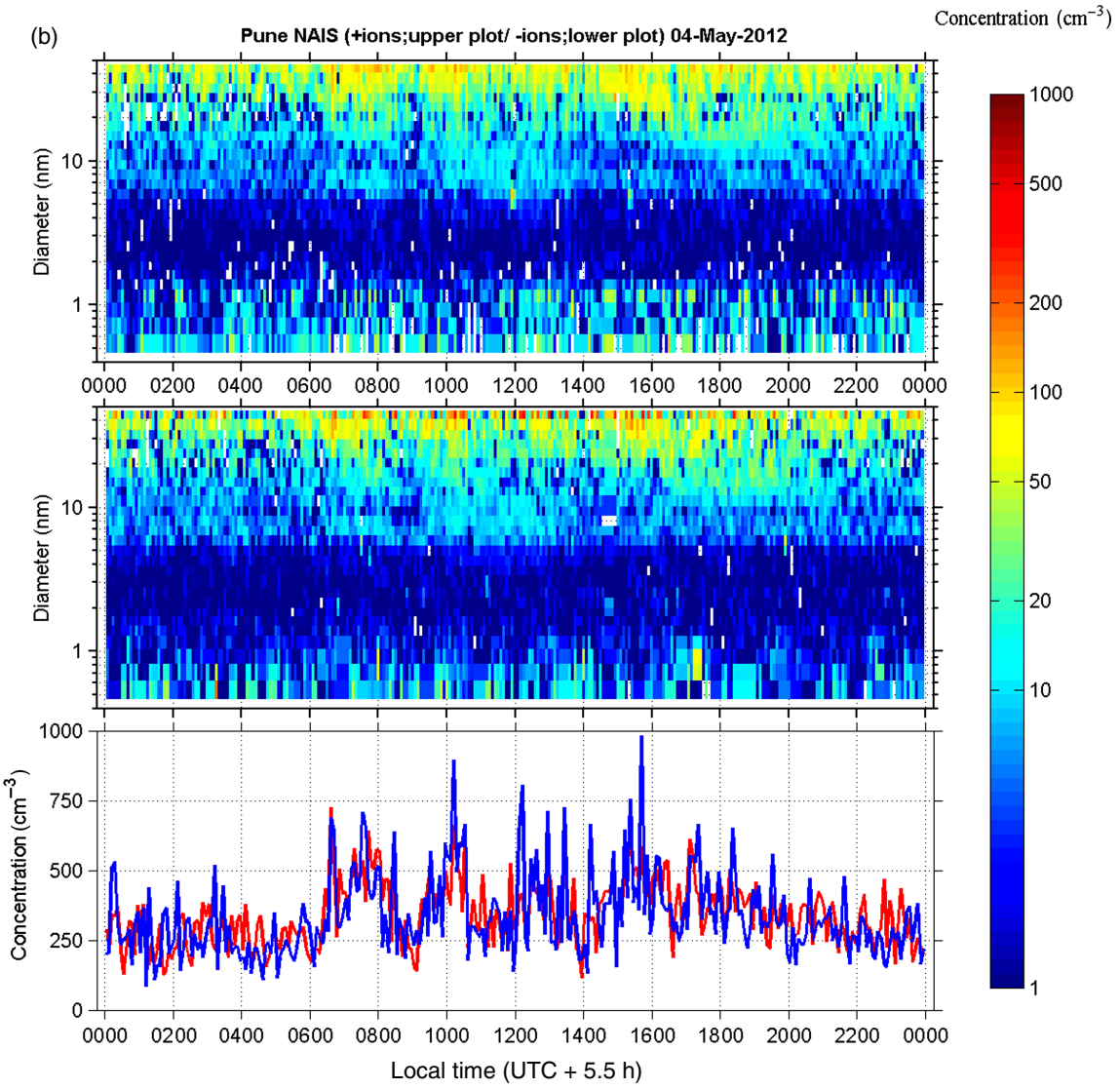

Figure 6. Continued.

measured by NAIS and SMPS, respectively, on 2 May 2012. The size range of ∼3.85–47.8 nm was covered in simultaneous measurements of both instruments. This unique dataset has been used here to study change in characteristics of ions and particles and their interactions during the NPF events. Although, the ion concentrations measured with NAIS at the sizes greater than 25 nm may be in error due to the multiple charged particles (Mirme and Mirme, 2013), such an error is not likely to be large. Moreover, whenever desirable, we have derived and discussed our results separately in 3.85–25 and 25–47.8 nm size categories.

The size-distribution functions, dn/dlog$D$, of small and big cluster ions (<1.7 nm) in Figure 8, soon after the generation of ions under stratified conditions at night-time, keep decreasing with the ion diameter, from 2000 to 0900 LT, presumably by recombination of oppositely charged ions and/or their conversion to large ions by attachment to aerosol particles. The minimum value of dn/dlog$D$ for ions then starts increasing with diameter at a comparatively faster rate. This faster rate of increase in dn/dlog$D$ for ions from 2000 to 0900 LT in Figure 8 is confined to the ions in the size range of 1.6–7.4 nm and is most probably associated with the formation/advection of intermediate ions in the morning hours. After attaining a peak at 7.4 nm, the dn/dlog$D$ values for ions experience a rapid but short fall but then again keep their increasing trend, though at a rate slower than that of ions of diameter from 1.6 to 7.4 nm. The short fall at 7.4 nm diameter shows that although the formation of intermediate ions ceases at this size which is the upper size-limit of this ion category, their dissipation by recombination/combination processes continues. This trend in ion distribution was observed on all days of the NPF events during our observation period. Concentration of aerosol particles in the common size range always remained higher than that of ions of the same size (Figure 8). However, the ions soon get attached to the aerosol particles and coagulation rate of these charged particles is relatively stronger than that of neutral particles for smaller size particles in this size range because of the larger electrostatic force contribution to the relative motion of charged particles. Yu and Turco (2001) determined that coagulation kernel (rate coefficient) is enhanced by a factor 10^3 for oppositely charged particles of radii 1 nm as compared with neutral particles. This enhancement in the coagulation rate contributes to higher rate of growth of smaller particles and may account for the much faster growth of such particles during the NPF event. However, this effect of charge on coagulation rate decreases fast as the particle size increases (Yu and Turco, 2001). The enhancement factor is already smaller than 5 for 3 nm particles (Yu and Turco, 2011). The small ions can also grow at rates comparable to coagulation rates, through ion–molecule reactions since the charged molecular recombination coefficient is 10^4 times greater than that for neutral molecules (Landau and Lifshitz, 1980). These changes in growth rates of ions and particles lead to their increase in size but decrease in concentration (due to their coagulation), and consequently to the development of a dip in dn/dlog$D$ values

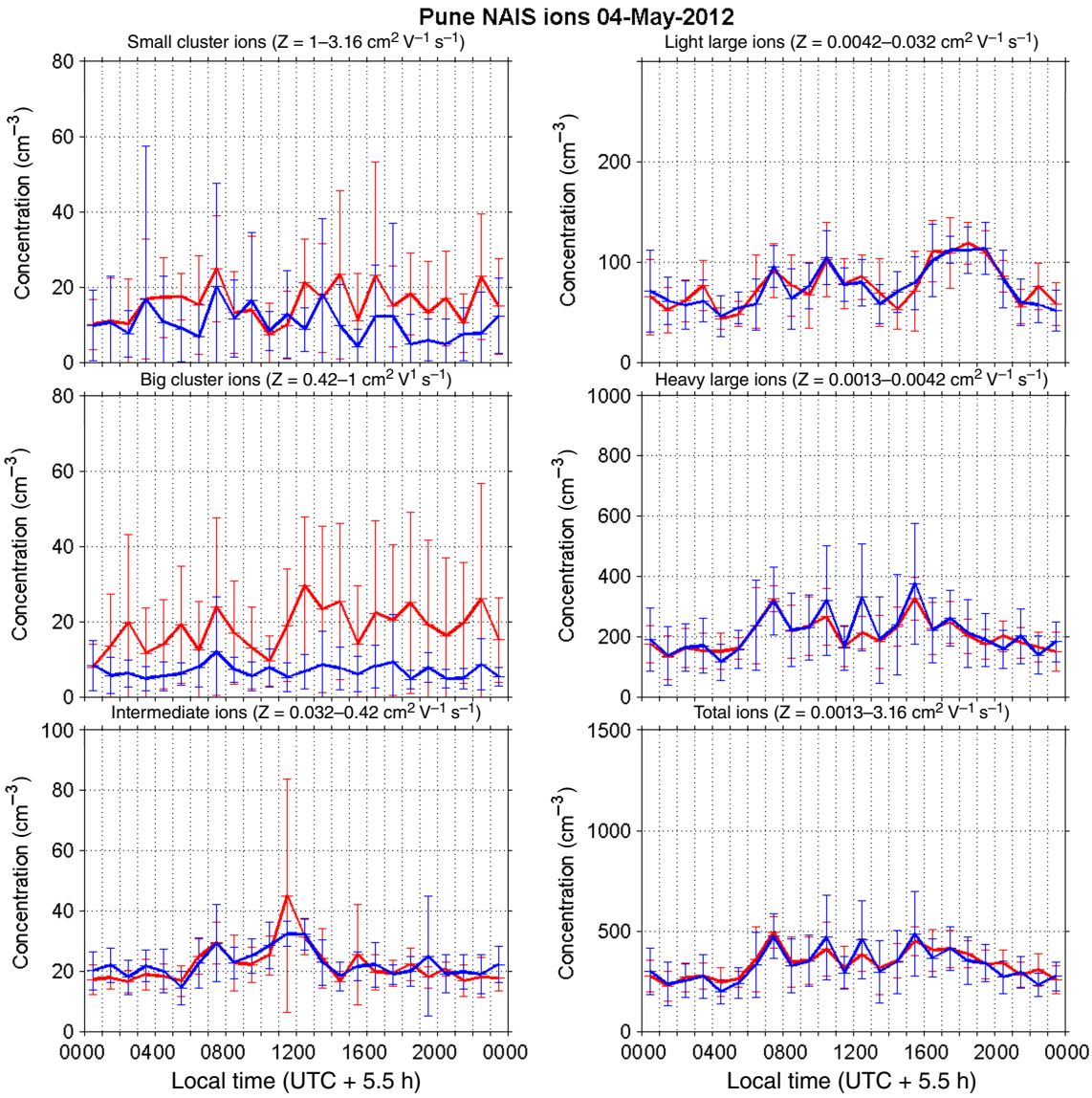

Figure 6. Continued.

Table 1. Average growth rates (GR) with their standard deviations for positive and negative ions of 3.9–25.3 nm (25.3–47.1 nm) diameter and particles of 3.85–25 nm (25–47.8 nm) diameter, percentage increase of GR of the positive/negative ions with respect to particles, and formation rate (J_5) of particles during the NPF event days.

Date in 2012 (time of start of NPF event, LT)	GR for ions (nm h^{-1})		GR for aerosol particles (nm h^{-1})	Increase of GR of ions over aerosol particles (%)		J_5 (cm^{-3} s^{-1})
	Positive	Negative		Positive	Negative	
23 April	8.6 ± 2.4	9.1 ± 2.8	8.1 ± 2.7	6.2	12.3	13.9
(0905)	(5.3 ± 1.6)	(5.4 ± 2.6)	(4.4 ± 1.8)	(20.5)	(22.7)	
28 April	7.3 ± 1.7	7.1 ± 1.8	6.1 ± 1.8	19.6	16.4	3.9
(1045)	(3.3 ± 1.4)	(3.1 ± 1.2)	(2.9 ± 1.3)	(13.7)	(6.8)	
30 April	7.5 ± 1.3	7.9 ± 2.1	6.4 ± 1.8	17.2	23.4	4.7
(1155)	(3.1 ± 1.8)	(3.5 ± 1.7)	(2.8 ± 0.9)	(10.7)	(25.0)	
1 May	8.8 ± 2.6	9.1 ± 2.6	7.4 ± 2.7	18.9	23.0	6.3
(1202)	(5.1 ± 2.1)	(6.7 ± 1.4)	(4.3 ± 1.9)	(18.6)	(55.8)	
2 May	10.7 ± 4.7	11.1 ± 3.7	9.8 ± 3.9	9.2	13.3	6.6
(0914)	(7.6 ± 4.5)	(8.9 ± 3.5)	(6.6 ± 2.2)	(15.20)	(34.8)	
10 May	7.8 ± 2.2	8.1 ± 2.5	7.4 ± 2.5	5.4	9.5	11.0
(0840)	(5.6 ± 1.9)	(5.9 ± 2.4)	(4.2 ± 1.3)	(33.3)	(40.5)	
12 May	5.8 ± 2.4	6.1 ± 3.1	5.2 ± 1.9	11.5	17.6	3.5
(0955)	(3.9 ± 1.3)	(4.1 ± 2.5)	(3.3 ± 2.4)	(18.1)	(24.2)	
22 May	10.3 ± 4.2	10.9 ± 4.5	8.9 ± 4.1	16.9	22.5	5.5
(0855)	(7.3 ± 2.4)	(7.6 ± 3.5)	(5.9 ± 2.4)	(23.7)	(28.1)	
23 May	8.9 ± 3.1	8.3 ± 2.6	7.1 ± 2.6	25.4	16.9	6.1
(0842)	(5.3 ± 2.9)	(5.7 ± 2.8)	(3.3 ± 2.2)	(60.6)	(72.7)	

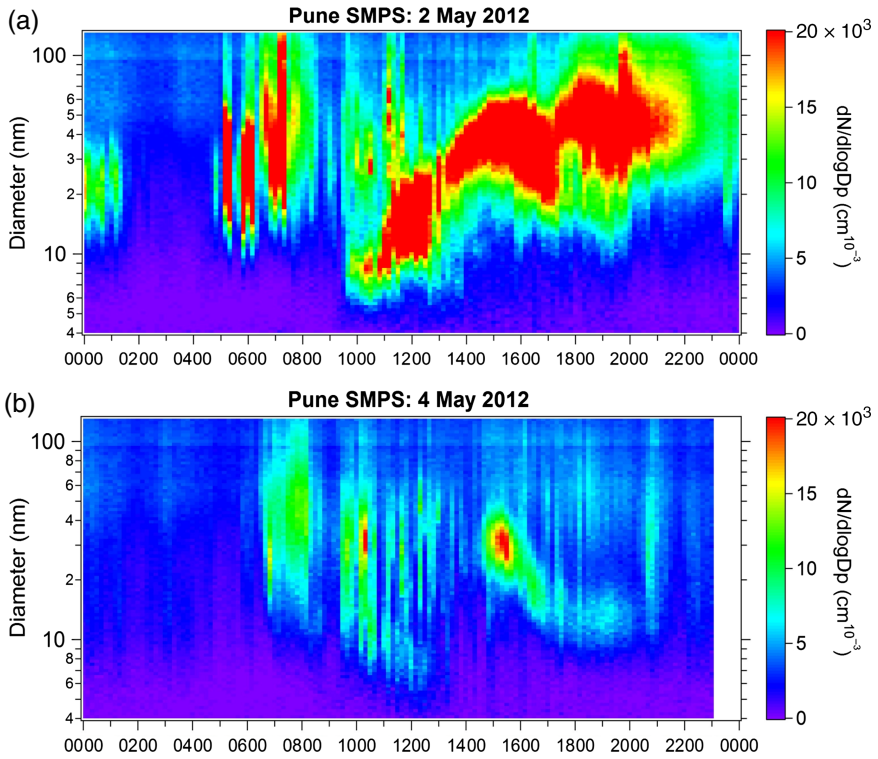

Figure 7. Diurnal variations of aerosol particle size spectra on (a) 2 May 2012 and (b) 4 May 2012.

Table 2. Condensation sink due to 4–135 nm diameter particles for observed NPF events at Pune in 2012. CS_{start} is the condensation sink at the start of the NPF event (i.e. at about 0900 LT). CS_{avg} is the condensation sink averaged over an NPF time duration of 0900–1600 LT.

Date	CS_{start} (10^{-3} s^{-1})	CS_{avg} (10^{-3} s^{-1})
23 April	9.2	8.4 ± 2.8
28 April	5.2	5.8 ± 0.7
30 April	4.2	5.9 ± 2.1
1 May	8.9	4.3 ± 1.6
2 May	2.7	5.1 ± 1.7
10 May	5.3	7.7 ± 1.0
12 May	4.9	6.4 ± 2.5
22 May	4.5	8.5 ± 3.6
23 May	4.4	7.3 ± 2.7

for particles in the size range of 3.85–7.4 nm diameter. This dip in dn/dlog$D$ values starts to develop at ∼2000 LT and continues to appear till ∼1000 LT (Figure 8(a,b)). Notably, this dip, i.e. a decrease followed by an increase in dn/dlog$D$ for particles and the peak in dn/dlog$D$ for ions, occurs in the same size range, thereby strongly indicating that ions combine with particles in this size range at a faster rate and convert them to charged particles (Yu and Turco, 2001). These charged particles grow much faster in size than the particles existing before these are charged during NPF events, strongly suggesting that either a larger fraction of particle population is charged and/or some of these particles carry multiple charges.

In addition to ion–particle attachment, ion–ion recombination also occurs at a faster rate due to enhanced concentrations of ions and particles during the NPF events. As a net effect of these and perhaps other processes, such as advection with winds during PECIA, concentrations of ions and particles become approximately equal to each other sometime during 0400–0800 LT. It is worth noting that, while the position of ion peaks in Figure 8 remains almost fixed at 7.4 nm or shifts towards higher size, the position of minima in particles dip shows some displacement from 6 nm towards a smaller size from 2000 to 1000 LT.

At about 1000 LT in Figure 8, a quick and more than tenfold increase occurs in concentration of the particles with diameters between 7 and 8 nm. As shown in Figure 7(a) this increase is associated with the enhanced rate of formation of new particles of this size during the NPF event. The shift of the mode diameter from 7–8 nm at 1000–1100 LT to ∼40 nm at 1600–1700 LT in Figure 8(a) well illustrates the growth of particles. The growth of particles occurs due to condensation of vapours and coagulation of particles. However, coagulation of particles is important in the atmosphere because it leads to a shift in the particle size distribution to larger size and reduces the build-up of very high concentrations of ultrafine particles produced during the NPF events (Harrison and Carslaw, 2003).

Figure 9 shows the diurnal variations of mode diameters of aerosol particles and ions of both polarities and condensation sink calculated from the data collected at 5 min resolution on 2 May 2012. The decrease in condensation sink from ∼0700 to 0900 is most likely associated with breakdown of nocturnal inversion and dispersion of ions and aerosols to higher levels. Such a decrease in condensation sink may help in creating necessary conditions for the occurrence of NPF at ∼0900 LT. An outstanding feature of this figure is a rapid and large decrease in mode diameter of the SMPS-measured particles accompanied by a rapid increase in condensation sink just after the start of the NPF event. An hour later, during 1000–1400 LT, measured negative ions also show downward peaks. During this period, condensation sink, in addition to showing two sharp peaks at ∼1000 LT, also shows an increasing trend. The absence of these peaks in the smooth curves in Figure 8 is due to a larger averaging period used for computing the data for the curves in Figure 8 than in Figure 9. Such trends in changes of ions, particles and condensation sink were observed in all the NPF events observed by us during our campaign period. These simultaneous but opposite changes, occurring in mode diameters of ions and particles on the one hand and condensation sink on the other, can very well be understood when one considers the burst of ultrafine particles during the NPF event. This addition of ultrafine particles will initially decrease the mode diameters of

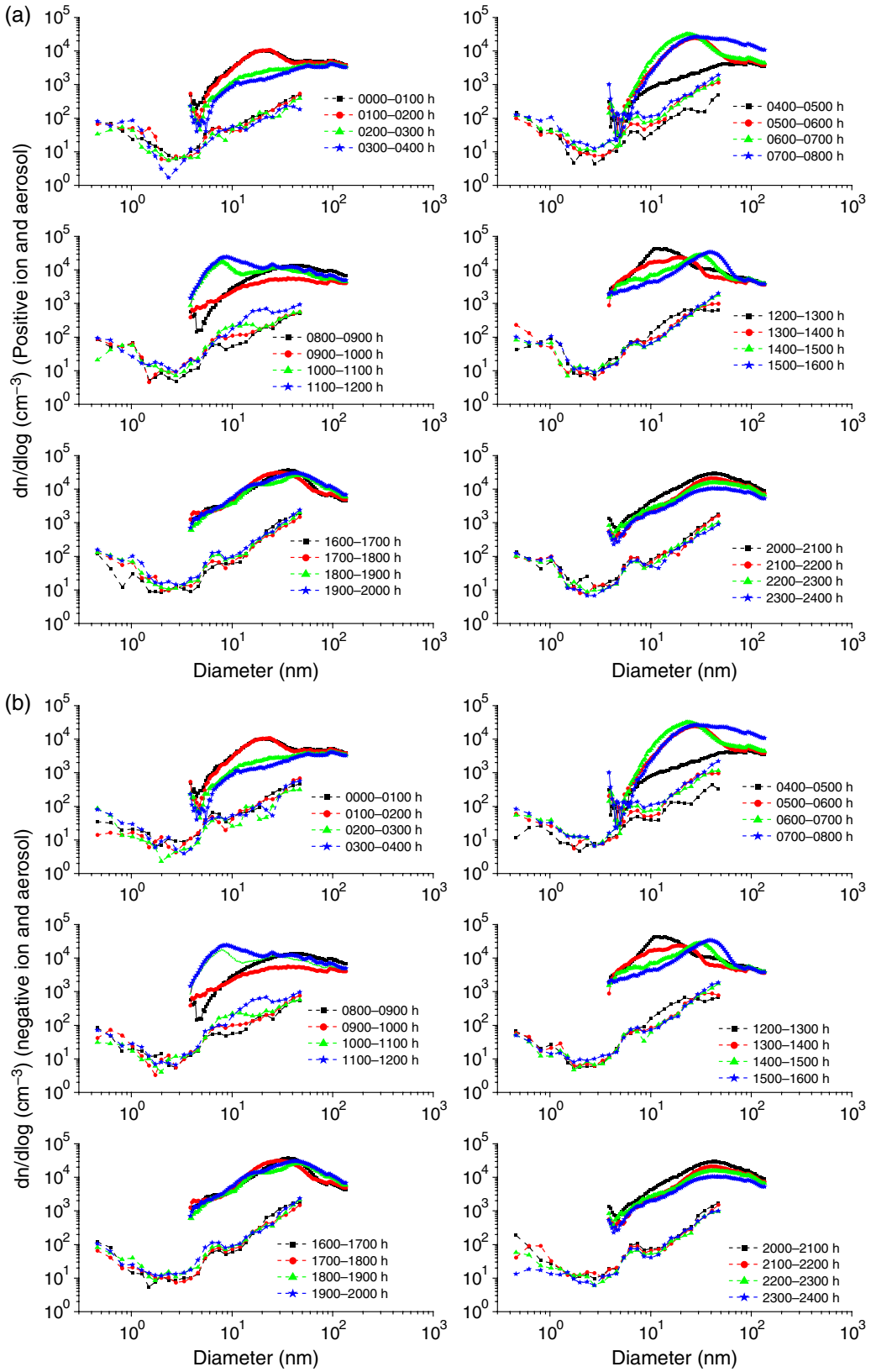

Figure 8. (a) The hourly-averaged number size distributions (dN/dlog$D$) of positive ions and aerosol particles on 2 May 2012. Dashed lines show variations of ions and continuous lines show variations of particles. (b) As in (a) for negative ions.

ions and particles but will cause an increase in condensation sink. However, these ultrafine ions and particles grow fast and after some time start contributing to the increase in mode diameter as well as to an increase in condensation sink. Another important feature of Figure 9 is that variation in mode diameters of ions of both polarities are roughly similar but always greater than that of particles at the start of the NPF event and continue to remain greater throughout the NPF event. This trend was universally observed during all the NPF events observed in our campaign period and strongly suggests that the mechanisms responsible for the growth of ions and aerosols are the same/similar and are not affected whether the particles are charged or uncharged. These observations also show that these ions have already grown to a mode diameter of ∼8 nm before the growth of both ions and particles starts during the NPF event. Since ions have already grown bigger than particles during PECIA and their growth rates during the NPF period are similar, the growth curve for the ions remains higher than the growth curve for particles during the NPF period.

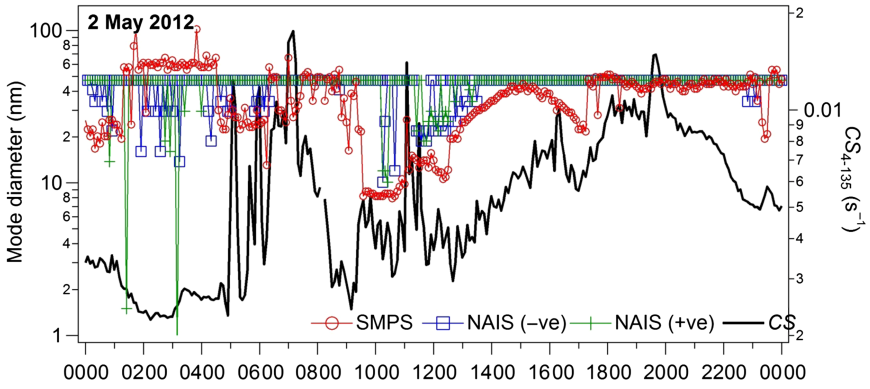

Figure 9. Diurnal variations (LT) of mode diameter of ions (both polarities), aerosol particles and condensation sink on 2 May 2012.

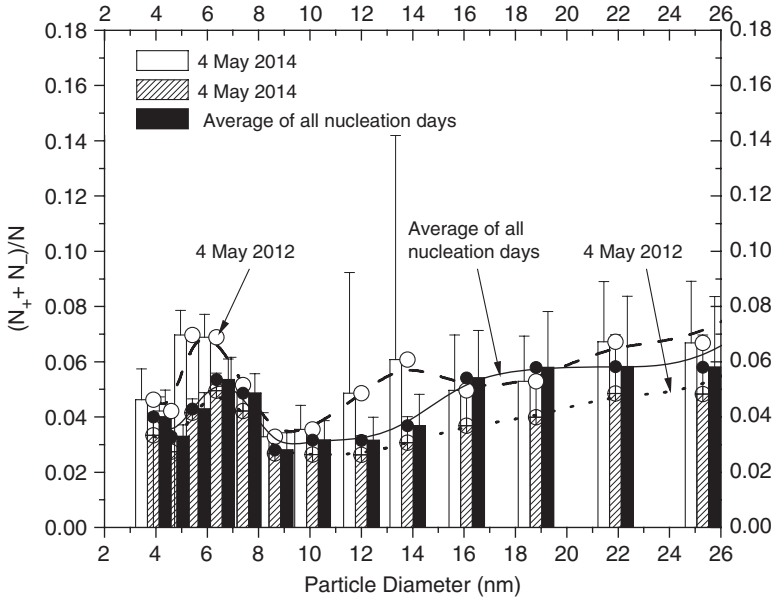

Figure 10. Variations of $(N_+ + N_-)/N$ with diameter for particles in the size range of 3.85–25.3 nm on 2 and 4 May 2012 and average of all event days during NPF events.Vertical bars show the standard errors. Curves are drawn by B-spline method during NPF events fitting the data on 2 and 4 May, and average values for all the event days.

3.6. *Ion–particle interactions*

The small ions of opposite polarity either recombine and neutralize each other or get attached to particles and are converted to large ions. In addition, an ion loss due to small ion deposition occurs as found by Hõrrak *et al.* (2008) in their measurements made in a coniferous forest. In this section, we aim to investigate the variability of the charged fraction for different particle sizes and under different environmental conditions prevailing over different periods of the NPF days when the formation, dissipation and transportation processes of the particles may differ.

To derive the relative importance of ion and neutral nucleation processes, it is useful to examine the overcharging of particles of <3 nm diameter. However, it is not possible to arrive at this ratio from our observations in view of: (i) the non-availability of data on neutral particles of <3 nm diameter, and (ii) the absence of any systematic and sustained growth rate of ions of <3 nm diameter. Instead, we have computed the ratio of total number of ions of both polarities $(N_+ + N_-)$ and total number of particles (N) in the size range of 3.9–25.3 nm diameter obtained from our data obtained from NAIS and SMPS measurements on all event days. Smooth curves in Figure 10 show variations of the ratio with particle diameter in the three cases. Approximately similar variations of this ratio for 2 May 2012 and for the average of all the NPF event days in Figure 10 confirm the typical nature of the event on 2 May 2012. The values of the charging ratio in these two curves for event days, especially for small particles (<14 nm), are much closer to each other than on non-event days. In view of the non-availability of data for <3 nm particles, an accurate quantitative assessment of overcharging of particles in this size range is not possible. However, it appears that about 3% of 3–4 nm particles are charged, which is higher than the ion equilibrium charge fraction of 1% (Reischl *et al.*, 1996). Moreover, the curves show a trend of attaining higher values of the ratio for particles <3 nm. This overcharging is an indication of the dominance of ion nucleation. Further, since particles >5 nm are known to soon (within a few seconds) achieve a charge equilibrium with ambient ions during NPF events (Laakso *et al.*, 2007; Gagné *et al.*, 2008; Yu and Turco, 2011), non-observation of such equilibrium in our observations indicates that such advected ions and particles are still in a state of evolution of charge equilibrium.

Figure 11 shows the diurnal variations of the $N/N_\pm$ for particles of different sizes on 2 May 2012. The ratio of $N/N_\pm$increases during both PECIA (maxima at 0600 LT) and NPF events (maxima at ~1000–1300 LT). The depression between these two maxima can be associated with the time interval between occurrence of PECIA and NPF events. The peak at 0100 and the depression between 0200 and 0400 LT are most likely to be associated with variability in the nocturnal process of particle formation and growth (Lee *et al.*, 2008; Boulon *et al.*, 2010; Ortega *et al.*, 2012; Kecorius *et al.*, 2015). It is notable in Figure 11 that enhancement in values of $N/N_\pm$ corresponds to relatively bigger

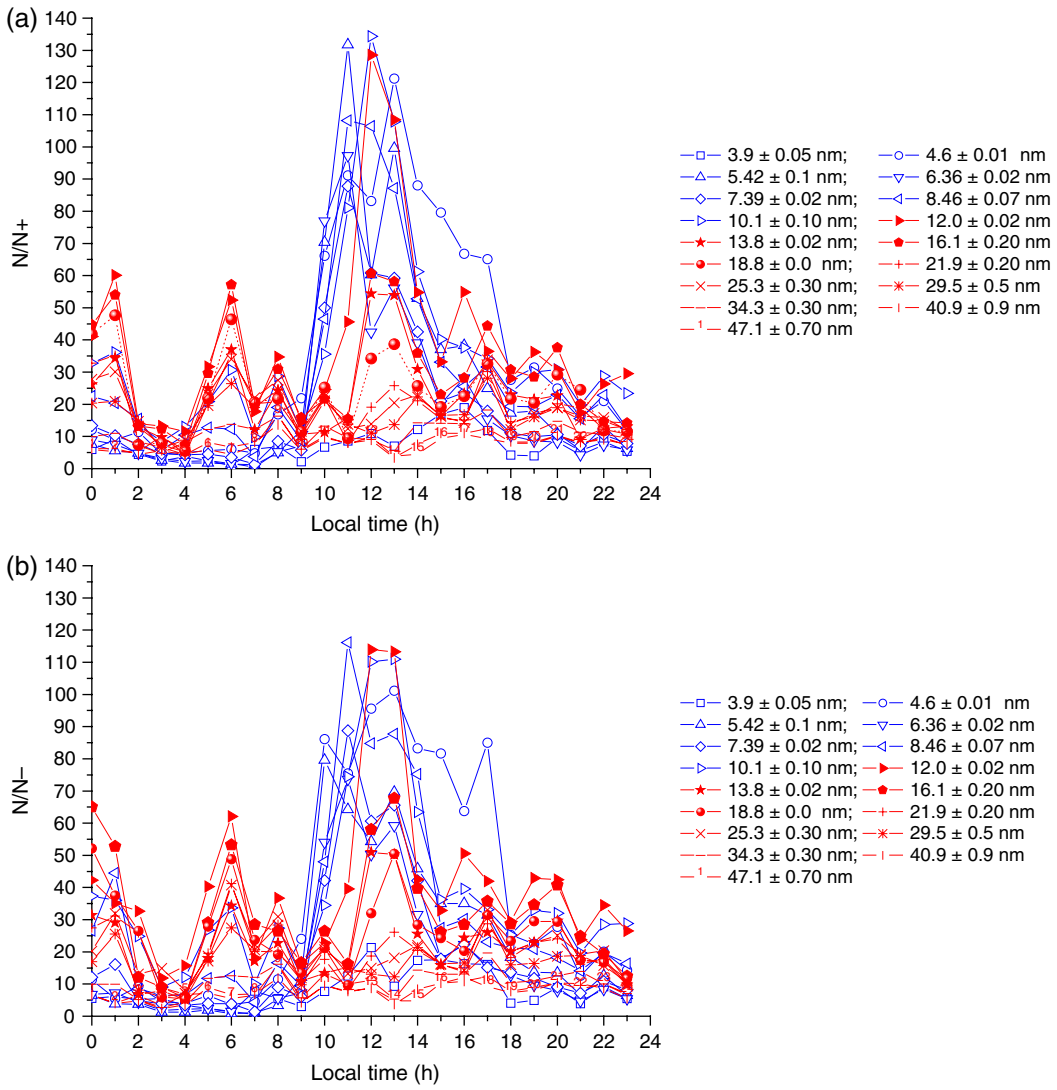

Figure 11. Diurnal variations of (a) N/N_+ and (b) N/N_- for particles of different sizes on 2 May 2012. Blue lines join the hollow symbols for particles of <12 nm diameter and red lines join the solid symbols for particles of ≥12 nm diameter.

ions and particles (∼16–25 nm) during PECIA and smaller ions and particles (∼4.6–12 nm) during the NPF period. However, it needs to be emphasized here that event modelling results of Yu and Turco (2011) show that the question of whether ion nucleation or neutral cluster mechanism is operating should be examined with the charged fraction at 1 nm diameter. Comparatively lower values of $N/N_\pm$ for particles in the intermediate size range during PECIA in the early morning hours indicate that either attachment of ions to the neutral particles plays a stronger role in their formation or a higher proportion of ions than neutral particles are advected to the measuring site during this period.

4. Discussion

Our observations provide a good dataset to study the ion–aerosol particle interactions and influence of the local topography and environmental conditions on characteristics of such interactions. The ions, aerosols, radioactive decay products and precursor gases accumulate below the stratified inversion layer formed at night-time near the Earth's surface along the hill-slopes (Porstendörfer, 1994). The transfer and accumulation of these elements at the measuring site increases and is maximum in the early morning hours when the solar rays first hit the surrounding hill-tops and set the katabatic winds flowing down the slopes of the hills surrounding the measuring site. It is worth noting that winds of ∼5 m s^{-1} flowing at ∼0600 LT quickly change their direction from northerly to southeasterly (Figure 4) in which direction the hills are closest to the measuring site. These winds bring down these elements accumulated along the hill-slopes. Observation of a high peak in ionization rate at about 0600 LT in our radon measurements (Figure 4) strongly indicates such downward advection of radon along the hill-slopes at the measuring site. Supporting such a transport are earlier observations of peaks in ion concentration and electrical conductivity (Dhanorkar and Kamra, 1993) and radon concentration (Kamsali *et al.*, 2011) in the early morning hours at the Atmospheric Electricity Observatory, located ∼100 m from this site which also reported similar accumulations of ions and radon and were explained by a similar transport mechanism.

Coagulation and removal of aerosol particles by scavenging also are largely enhanced if the particles are electrically charged by artificial or natural ionization (Clement *et al.*, 1995; Tripathi and Harrison, 2001). Ionization can also produce ultrafine particles either by clustering of water molecules around ions or from homogeneous nucleation of H_2SO_4 or HNO_3 generated radiolytic reactions at typical levels of natural radioactivity (radon) in the atmosphere (Vohra *et al.*, 1984). Growth of such ions/particles has been suggested as providing a source of cloud condensation nuclei (Yu and Turco, 2001). These model results suggest that most of these particles are those derived from original charged clusters and therefore the ion-mediated particle formation mechanism is likely to be most important in the lower atmosphere. Our observations

of a rapid increase in ion concentration of intermediate category and greater growth rates of ions of both polarities than those of neutral particles (Figure 8(a,b)) support the theory that the formation and growth of ions below the inversion layer occurs by the ion-mediated nucleation mechanism and/or advection of ions with katabatic winds during PECIA when the solar radiation is absent or very low in the early morning hours. Further, our measurements also support model results of ion-mediated nucleation theory (Yu and Turco, 2000, 2001; Yu, 2003), which show that the charged molecular clusters, formed around ions, are much more stable and can grow faster than corresponding neutral clusters and can preferentially achieve stable sizes. Model results of Nadykto and Yu (2003) also show that the interaction of charges with polar gas molecules enhances the growth rate of small charged clusters. These results are important because if the ions/particles can grow to the size of cloud condensation nuclei, they can affect cloud formation and possibly cause a change in climate (Carslaw *et al.*, 2002).

Positively charged ions and particles tend to settle down to the Earth's surface under the electrical forces in the early morning hours. The resulting reduction of the surface area of the pre-existing aerosol particles will cause a reduction in condensation sink which combined with the increasing solar radiation and ionization (Figures 4 and 5) in the morning hours contribute to creating suitable conditions for the occurrence of NPF events which normally occur at this location between 0830 and 1200 LT. The large decrease in condensation sink between 0700 and 0900 LT on 2 May 2012 (Figure 9) and lower values of CS_{start} than CS_{avg} observed during most of the events (in Table 2) confirm such low values of the surface area of the pre-existing particles at ∼0900 LT.

Formation of intermediate ions during the NPF events causes a rapid enhancement in ion concentration in the size range of 1.7–7.4 nm (Figure 8). These intermediate ions, in addition to the existing small ions, get attached to neutral particles, reduce their concentration, and convert them to large/intermediate ions (Figure 8). Under the net effect of ion–aerosol attachment, ion–ion recombination and perhaps other processes such as advection, concentrations of ions and aerosols become almost equal to each other during 0400–0800 LT (Figure 8). Thus Boltzmann charge distribution of particles in this size range breaks down during such periods. Breakdown of Boltzmann charge distribution for particles below 100 nm has also been reported by Hussin *et al.* (1983) and Hoppel and Frick (1986).

In most of the banana-type NPF events reported at different locations around the world, growth of particles starts from the molecular or cluster size particles which are formed by the nucleation process (e.g. Kulmala *et al.*, 2004). In our observations of the NPF events, the growth of particles starts from the size of 4 to 6 nm. It is uncertain, however, how particles grow to such sizes even before the NPF events. We propose that particles of this size (4–6 nm) are provided from the remnants of PECIA events. These particles may be charged/uncharged aerosol particles which accumulate along the hill-slopes and grow by electrostatic force during night-time to the size of 4–6 nm and are then transported downwards through to the stratified atmospheric boundary layer during the PECIA events by the katabatic winds in the early morning. The model results, that most of the large particles grown up after a few hours are those derived from original charged clusters, support our hypothesis (Yu and Turco, 2001, 2011). Figures 6 and 7 do show some enhanced concentrations of 60–85 cm^{-3} for the sum of intermediate ions of both polarities and particles, respectively, during the PECIA period. The intermediate ions formed during the NPF events may get attached to particles or ions and may cause formation of singly or multiply charged aerosol particles. The resulting charged fraction of particles will have greater growth rate (Clement *et al.*, 1995; Tripathi and Harrison, 2001). It is significant to note that night-time observations of Lee *et al.* (2008) of such periods of high concentrations of ultrafine particles also report particles of 4–9 nm diameters. Although no particular mechanism for night-time events of particle formation is identified, their occurrence may be important for aerosol generation and the radiation budget on a global scale that may eventually affect the climate.

Higher values of charge fraction of 3–4 nm diameter particles in our observations than their equilibrium values indicate the dominance of ion nucleation. On the other hand, our observations of non-observation of a systematic and sustained growth pattern of ions of <3 nm diameter during PECIA and non-observation of charge equilibrium for particles >5 nm in our observations support the advection of ions and particles. The present observations are not detailed enough to assess relative contributions of these processes. Comparatively lower values of $N/N_{\pm}$ during PECIA than in NPF events indicate either a stronger role of ion–particle attachment processes and/or dominance of ions over aerosol particles in the katabatic airflow during PECIA.

5. Conclusions

Our simultaneous measurements of ions and aerosol particles in the size range of 3.85–47.8 nm diameter show that the ion–aerosol particle interactions at this site are strongly influenced by the local topography and environmental conditions. Major characteristics are described below:

1. During the nine truncated banana-type NPF events observed during our campaign period: (i) the average rate of formation of 5 nm diameter particles were observed to range between 3.9 and 13.9 cm^{-3} s^{-1}, and (ii) the average rate of growth ranged between 5.2 and 9.8 nm h^{-1} for particles in the size range of 3.85–25 nm but only between 2.8 and 5.9 nm h^{-1} for particles in the size range of 25–47.8 nm. These values are, however, subject to the same uncertainties as discussed in section 3.3.
2. During the same NPF events, average rates of growth of positive (negative) ions ranged between 5.8 and 10.7 (6.1 and 11.1) nm h^{-1} for ions in the size range of 3.9–25.3 nm and between 3.1 and 7.6 (3.1 and 8.9) nm h^{-1} for ions in the size range of 25.3–47.8 nm. So, growth rates of positive (negative) ions were 5.1–25.3% (1.1–60.6%) higher than for particles in the size range of 3.9–25.3 nm and 9.5–22.5% (9.6–55.8%) higher than for particles in the size range of 25.3–47.8 nm.
3. Total ion concentrations were approximately double on event days than on non-event days.
4. The NPF events are generally preceded by 2–3 h by PECIA. Large concentrations of ions, particles, radon and condensing vapours accumulated below inversion layers during the PECIA encourage ion nucleation and growth of ultrafine ions. In addition, small and cluster ions, during their downward journey with katabatic winds along the hill-slope, recombine and combine with neutral particles and grow in size at a rate faster than the neutral particles. As a result, ions attain a mode diameter greater than those of uncharged particles (Figure 9). However, this faster rate of ion growth continues only up to a size of ∼8 nm. Therefore, ions attain a diameter greater than

that of neutral particles even before the start of the NPF events. Availability of these larger-than-neutral charged particles at the beginning of the NPF events is reflected in our observations (Figure 9). So, remnants of PECIA in the early morning period provide ions already grown to the size of 4–8 nm diameter for their further growth during the NPF events. During the NPF event, mode diameters of these ions and particles, after having an initial large and steep fall, increase at approximately the same rate (Figure 9). This large and steep fall in mode diameters of these ions and particles is accompanied by an equally large and steep increase in condensation sink.

5. Ions in the intermediate size range attach with aerosol particles. As a net result of the ion–ion recombination, ion–aerosol particle attachment, and other processes such as advection, concentrations of ions and particles in this size range become almost equal to each other during 0400–0800 LT. Thus Boltzmann charge distribution breaks down for particles in this size range.
6. The settling of positively charged ions and particles under electric force, the breaking of the nocturnal inversion and the weakening of katabatic winds at ∼0700–0800 LT reduce the fresh induction of ions and particles and dispersion of ions and particles to higher levels, and thus contribute to a large reduction in the particle mode diameters. This results in a decrease in condensation sink and helps in creating conducive conditions for the occurrence of NPF.
7. The observation that the charging ratio of 3–4 nm particles is higher than their charge equilibrium values indicates occurrence of ion nucleation during PECIA. However, the observation that particles >5 nm do not attain charge equilibrium indicates that either such particles grow too fast to obtain the equilibrium or the advection of ions and particles.
8. Mode diameter of particles shifts from 7–8 nm at 1000–1100 LT to ∼40 nm at 1600–1700 LT and the growth is most probably mainly due to condensation of vapours, and/or coagulation of particles.

Acknowledgements

The authors thank B. N. Goswami (Director, IITM) for his support and encouragement during this study and observation campaign at Pune and gratefully acknowledge the funding support from the Ministry of Earth Sciences (MoES). They also thank the India Meteorological Department Observatory at Pune for providing the meteorological data. We acknowledge NOAA ARL for providing HYSPLIT air mass back-trajectory calculations (http://www.arl.noaa.gov/ready.html). DS and ASG thank K. Komsaare, University of Tartu, Estonia for his help in computer programming for analysing the ion spectrometer data. AKK acknowledges the support under the INSA Senior Scientist and INSA Honorary Scientist Programmes. The authors wish to thank the anonymous reviewers for their suggestions which helped to improve the article.

References

Anderson R. 1965. Electricity in volcanic clouds: Investigations show that lightning can result from charge-separation processes in a volcanic crater. *Science* **148**: 1179–1189, doi: 10.1126/science.148.3674.1179.

Betha R, Spracklen DV, Balasubramanian R. 2013. Observations of new aerosol particle formation in a tropical urban atmosphere. *Atmos. Environ.* **71**: 340–351.

Blanchard DC. 1963. Electrification of the atmosphere by particles from bubbles in the sea. *Prog. Oceanogr.* **1**: 71–202.

Boulon J, Sellegri K, Venzac H, Picard D, Weingartner E, Wehrle G, Collaud Coen M, Bütikofer R, Flückiger E, Baltensperger U, Laj P. 2010. New particle formation and ultrafine charged aerosol climatology at high altitude site in the Alps (Jungfraujoch, 3580 m a.s.l., Switzerland). *Atmos. Chem. Phys.* **10**: 9333–9349.

Carslaw KS, Harrison RG, Kirkby J. 2002. Cosmic rays, clouds and climate. *Science* **298**: 1732–1737.

Chalmers JA. 1967. *Atmospheric Electricity*. Pergamon Press: London.

Clement CF, Clement RA, Harrison RG. 1995. Charge distributions and coagulation of radioactive aerosols. *J. Aerosol Sci.* **26**: 1207–1226.

Covert DS, Kapustin VN, Bates TS, Quinn PK. 1996. Physical properties of marine boundary layer aerosol particles of the mid-Pacific in relation to sources and meteorological transport. *J. Geophys. Res.* **101**: 6919–6930, doi: 10.1029/95JD03068.

Dal Maso M, Kulmala M, Riipinen I, Wagner R, Hussein T, Aalto P, Lehtinen EJ. 2005. Formation and growth rates of fresh atmospheric aerosols: eight years of aerosol size distribution data from SMEAR II, Hyytiälä, Finland. *Boreal Environ. Res.* **10**: 323–336.

Dhanorkar S, Kamra AK. 1993. Diurnal and seasonal variations of the small-, intermediate-, and large-ion concentrations and their contributions to polar conductivity. *J. Geophys. Res.* **98**: 14895–14908, doi: 10.1029/93JD00464.

Draxler RR, Rolph GD. 2010. *HYSPLIT (HYbrid Single-Particle Lagrangian Integrated Trajectory) Model*. NOAA Air Resources Laboratory: Silver Spring, MD. http://ready.arl.noaa.gov/HYSPLIT.php (accessed 15 October 2014).

Dunn MJ, Jimenez J-L, Baumgardner D, Castro T, McMurry PH, Smith JN. 2004. Measurements of Mexico City nanoparticle size distributions: observations of new particle formation and growth. *Geophys. Res. Lett.* **31**: L10102, doi: 10.1029/2004GL019483.

Eisele FL, Lovejoy ER, Kosciuch E, Moore KF, Mauldin RL III, Smith JN, McMurry PH, Iida K. 2006. Negative atmospheric ions and their potential role in ion-induced nucleation. *J. Geophys. Res.* **111**: D04305, doi: 10.1020/2005JD006568.

Gagné S, Laakso L, Petäjä T, Kerminen V-M, Kulmala M. 2008. Analysis of one year of Ion-DMPS data from the SMEAR II station, Finland. *Tellus* **60B**:: 318–329.

Gagné S, Nieminen T, Kurtén T, Manninen HE, Petäjä T, Laakso L, Kerminen V-M, Boy M, Kulmala M. 2010. Factors influencing the contribution of ion-induced nucleation in a boreal forest, Finland. *Atmos. Chem. Phys.* **10**: 3743–3757, doi: 10.5194/acp-10-3743-2010.

García MI, Rodríguez S, González Y, García RD. 2014. Climatology of new particle formation at Izaña mountain GAW observatory in the subtropical North Atlantic. *Atmos. Chem. Phys.* **14**: 3865–3881, doi: 10.5194/acp-14-3865-2014.

Gonser SG, Klein F, Birmile W, Gorob J, Kulmal M, Manninen HE, Wieldensohler A, Held A. 2014. Ion–particle interactions during formation and growth at a coniferous forest site in Central Europe. *Atmos. Chem. Phys.* **14**: 10547–10563.

Gopalakrishnan V, Deshpande CG, Kamra AK. 1996. Measurements of atmospheric electric field and conductivity in the locality of a gas well flame. *Geophys. Res. Lett.* **23**: 3615–3618, doi: 10.1029/96GL03150.

Gopalakrishnan V, Pawar SD, Siingh D, Kamra AK. 2005. Intermediate ion formation in the ship's exhaust. *Geophys. Res. Lett.* **32**: L11806, doi: 10.1029/2005GL022613.

Harrison RG, Aplin KL. 2001. Atmospheric condensation nuclei formation and high-energy radiation. *J. Atmos. Sol.-Terr. Phys.* **63**: 1811–1819.

Harrison RG, Carslaw KS. 2003. Ion–aerosol–cloud processes in the lower atmosphere. *Rev. Geophys.* **41**: 1012, doi: 10.1029/2002RG000114.

Hirsikko A, Paatero J, Hatakka J, Kulmala M. 2007. The ^{222}Rn activity concentration, external radiation dose and air ion production rate in a boreal forest in Finland between March 2000 and June 2006. *Boreal Environ. Res.* **12**: 247–264.

Hoppel WA, Frick GM. 1986. Ion–aerosol attachment coefficients and the steady-state charge distribution on aerosols in a bipolar environment. *Aerosol Sci. Technol.* **5**: 1–21.

Hoppel WA, Andersion RV, Willett JC. 1986. Atmospheric electricity in the planetary layer. In *Studies in Geophysics, The Earth's Electrical Environment,* Krider EP, Roble RG (eds.): 149–165. National Academy Press: Washington, DC.

Hõrrak U, Salm J, Tammet H. 1998. Bursts of intermediate ions in atmospheric air. *J. Geophys. Res.* **103**: 13909–13915, doi: 10.1029/97JD01570.

Hõrrak U, Salm J, Tammet H. 2003. Diurnal variation in the concentration of air ions of different mobility classes in a rural area. *J. Geophys. Res.* **108**: 4653, doi: 10.1029/2002JD003240.

Hõrrak U, Aalto PP, Salm J, Komsaare K, Tammet H, Mäkelä JM, Laakso L, Kulmala M. 2008. Variation and balance of positive air ion concentrations in a boreal forest. *Atmos. Chem. Phys.* **8**: 655–675, doi: 10.5194/acp-8-655-2008.

Hussin A, Scheibel HG, Becker KH, Porstendörfer J. 1983. Bipolar diffusion charging of aerosol particles. I: Experimental results within the diameter range 4–30 nm. *J. Aerosol Sci.* **14**: 671–677.

Kamra AK. 1969. Effect of wind on diurnal and seasonal variations of atmospheric electric field. *J. Atmos. Sol.-Terr. Phys.* **31**: 1281–1286.

Kamra AK. 1972a. Measurements of the electrical properties of dust storms. *J. Geophys. Res.* **77**: 5856–5869, doi: 10.1029/JC077i030p05856.

Kamra AK. 1972b. Visual observation of electric sparks on gypsum dunes. *Nature* **240**: 143–144, doi: 10.1038/240143a0.

Kamra AK. 1989. Charge transfer by point discharge below dust storms. *Geophys. Res. Lett.* **16**: 127–129, doi: 10.1029/GL016i002p00127.

Kamsali N, Pawar SD, Murugavel P, Gopakrishnan V. 2011. Estimation of small ion concentration near the Earth's surface. *J. Atmos. Sol.-Terr. Phys.* **73**: 2345–2351, doi: 10.1016/j/jastp.2011.07.011.

Kanawade VP, Tripathi SN. 2006. Evidence for the role of ion-induced particle formation during an atmospheric nucleation event observed in Tropospheric Ozone Production about the Spring Equinox (TOPSE). *J. Geophys. Res.* **111**: D02209, doi: 10.1029/2005JD006366.

Kanawade VP, Tripathi SN, Siingh D, Gautam AS, Srivastava AK, Kamra AK, Soni VK, Sethi V. 2014. Observations of new particle formation at two distinct Indian subcontinental urban locations. *Atmos. Environ.* **96**: 370–379, doi: 10.1016/j.atmosenv.2014.08.001.

Kecorius S, Zhang S, Wang Z, Größ J, Ma N, Wu Z, Ran L, Hu M, Wang P, Ulevičius V, Wiedensohler A. 2015. Nocturnal aerosol particle formation in the north China plain. *Lith. J. Phys.* **55**: 44–53.

Keefe D, Nolan PJ, Rich TA. 1959. Charge equilibrium in aerosols according to the Boltzmann law. *Proc. R. Irish Acad.* **A60**: 27–45.

Kerminen V-M, Pirjola L, Kulmala M. 2001.How significantly does coagulation scavenging limit atmospheric particle production? *J. Geophys. Res.* **106**: 24119–24125, doi: 10.1029/2001JD000322.

Kolarz P, Gaisberger M, Madl P, Hofmann W, Ritter M, Hartl A. 2012. Characterization of ions at Alpine waterfalls. *Atmos. Chem. Phys.* **12**: 3687–3697, doi: 10.5194/acp-12-3687-2012.

Korhonen H, Sihto S-L, Kerminen V-M, Lehtinen KEJ. 2011. Evaluation of the accuracy of analysis tools for atmospheric new particle formation. *Atmos. Chem. Phys.* **11**: 3051–3066, doi: 10.5194/acp-11-3051-2011.

Kulmala M, Pirjola L, Makela JM. 2000. Stable sulphate clusters as a source of new atmospheric particles. *Nature* **404**: 66–69.

Kulmala M, Dal Maso M, Mäkelä JM, Pirjola L, Väkevä M, Aalto P, Miikkulainen P, Hämeri K, O'Dowd CD. 2001. On the formation, growth and composition of nucleation mode particles. *Tellus* **53B**: 479–490.

Kulmala M, Vehkamaki H, Petäjä T, Dal Maso M, Lauri A, Kerminen V-M, Birmili W, McMurry PH. 2004. Formation and growth rates of ultrafine atmospheric particles: A review of observations. *J. Aerosol Sci.* **35**: 143–176.

Kulmala M, Petäjä T, Mönkkönen P, Koponen IK, Dal Maso M, Aalto PP, Lehtinen KEJ, Kerminen V-M.. 2005. On the growth of nucleation mode particles: Source rates of condensable vapor in polluted and clean environments. *Atmos. Chem. Phys.* **5**: 409–416.

Kulmala M, Lehtinen KEJ, Laaksonen A. 2006. Cluster activation theory as an explanation of the linear dependence between formation rate of 3 nm particles and sulphuric acid concentration. *Atmos. Chem. Phys.* **6**: 787–793.

Kulmala M, Petäjä T, Nieminen T, Sipilä M, Manninen HE, Lehtipalo K, Dal Maso M, Aalto PP, Junninen H, Paasonen P, Riipinen I, Lehtinen KEJ, Laaksonen A, Kerminen V-M. 2012. Measurement of the nucleation of atmospheric aerosol particles. *Nat. Protoc.* **7**: 1651–1667, doi: 10.1038/nprot.2012.091.

Kulmala M, Kontkanen J, Junninen H, Lehtipalo K, Manninen HE, Nieminen T, Petäjä T, Sipilä M, Schobesberger S, Rantala P, Franchin A, Jokinen T, Järvinen E, Äijälä M, Kangasluoma J, Hakala J, Aalto PP, Paasonen P, Mikkilä J, Vanhanen J, Aalto J, Hakola H, Makkonen U, Ruuskanen T, Mauldin RL III, Duplissy J, Vehkamäki H, Bäck J, Kortelainen A, Riipinen I, Kurtén T, Johnston MV, Smith JN, Ehn M, Mentel TF, Lehtinen KE, Laaksonen A, Kerminen VM, Worsnop DR. 2013. Direct observations of atmospheric aerosol nucleation. *Science* **339**: 943–946.

Laakso L, Gagné S, Petäjä T, Hirsikko A, Aalto PP, Kulmala M, Kerminen V-M. 2007. Detecting charging state of ultra-fine particles: Instrumental development and ambient measurements. *Atmos. Chem. Phys.* **7**: 1333–1345.

Laakso L, Laakso H, Aalto PP, Keronen P, Petäjä T, Nieminen T, Pohja T, Siivola E, Kulmala M, Kgabi N, Molefe M, Mabaso D, Phalatse D, Pienaar K, Kerminen V-M. 2008. Characteristics of atmospheric particles, trace gases and meteorology in a relatively clean southern African savannah environment. *Atmos. Chem. Phys.* **8**: 4823–4839.

Laaksonen A, Kulmala M, O'Dowd CD, Joutsensaari J, Vaattovaara P, Mikkonen S, Lehtinen KEJ, Sogacheva L, Dal Maso M, Aalto P, Petäjä T, Sogachev A, Yoon YJ, Lihavainen H, Nilsson D, Facchini MC, Cavalli F, Fuzzi S, Hoffmann T, Arnold F, Hanke M, Sellegri K, Umann B, Junkermann W, Coe H, Allan JD, Alfarra MR, Worsnop DR, Riekkola M-L, Hyötyläinen T, Viisanen Y. 2008. The role of VOC oxidation products in continental new particle formation. *Atmos. Chem. Phys.* **8**: 2657–2665.

Landau LD, Lifshitz EM. 1980. *Statistical Physics, Part 1* (3rd edn). Pergamon Press: New York, NY.

Lee S-H, Reeves JM, Wilson JC, Hunton DE, Viggiano AA, Miller TM, Ballenthin JO, Lait LR. 2003. Particle formation by ion nucleation in the upper troposphere and lower stratosphere. *Science* **301**: 1886–1889.

Lee S-H, Young L– H, Benson DR, Suni T, Kulmala M, Junninen H, Campos TL, Rogers DC, Jensen J. 2008. Observations of nighttime new particle formation in the troposphere. *J. Geophys. Res.* **113**: D10210, doi: 10.1029/2007JD009351.

Lehtipalo K, Kulmala M, Sipilä M, Petäjä T, Vana M, Ceburnis MD, Dupuy R, O'Dowd CD. 2010. Nanoparticles in boreal forest and coastal environment: a comparison of observations and implications of the nucleation mechanism. *Atmos. Chem. Phys.* **10**: 7009–7016, doi: 10.5194/acp-10-7009-2010.

Lida K, Stolzenburg M, McMurry P, Dunn MJ, Smith JN, Eisele F, Keady P. 2006. Contribution of ion-induced nucleation to new particle formation: Methodology and its application to atmospheric observations in Boulder, Colorado. *J. Geophys. Res.* **111**: D23201, doi: 10.1029/2006JD007167.

Lovejoy ER, Curtius J, Froyd KD. 2004. Atmospheric ion-induced nucleation of sulfuric acid and water. *J. Geophys. Res.* **109**: D08204, doi: 10.1029/2003JD004460.

Luts A, Parts T-E, Laakso L, Hirsikko A, Grönholm T, Kulmala M. 2009. Some air electricity phenomena caused by WFs: Correlative study of the spectra. *Atmos. Res.* **91**: 229–237.

McMurry PH, Fink M, Sakurai H, Stolzenburg MR, Mauldin RL III, Smith J, Eisele F, Moore K, Sjostedt S, Tanner D, Huey LG, Nowak JB, Edgerton E, Voisin D. 2005. A criterion for new particle formation in the sulfur-rich Atlanta atmosphere. *J. Geophys. Res.* **110**: D22S02, doi: 10.1029/2005JD005901.

Manninen HE, Nieminen T, Riipinen I, Yli-Juuti T, Gagné S, Asmi E, Aalto PP, Petäjä T, Kerminen V-M, Kulmala M. 2009a. Charged and total particle formation and growth rates during EUCAARI 2007 campaign in Hyytiälä. *Atmos. Chem. Phys.* **9**: 4077–4089.

Manninen HE, Petäjä T, Asmi E, Riipinen I, Nieminen T, Mikkilä J, Hõrrak U, Mirme A, Mirme S, Laakso L, Kerminen V-M, Kulmala M. 2009b. Long-term field measurements of charged and neutral clusters using Neutral cluster and Air Ion Spectrometer (NAIS). *Boreal Environ. Res.* **14**: 591–605.

Manninen HE, Nieminen T, Asmi E, Gagné S, Häkkinen S, Lehtipalo K, Aalto P, Vana M, Mirme A, Mirme S, Hõrrak U, Plass-Dülmer C, Stange G, Kiss G, Hoffer A, Törö N, Moerman M, Henzing B, de Leeuw G, Brinkenberg M, Kouvarakis GN, Bougiatioti A, Mihalopoulos N, O'Dowd CD, Ceburnis D, Arneth A, Svenningsson B, Swietlicki E, Tarozzi L, Decesari S, Facchini MC, Birmili W, Sonntag A, Wiedensohler A, Boulon J, Sellegri K, Laj P, Gysel M, Bukowiecki N, Weingartner E, Wehrle G, Laaksonen A, Hamed A, Joutsensaari J, Petäjä T, Kerminen V-M, Kulmala M. 2010. EUCAARI ion spectrometer measurements at 12 European sites – analysis of new particle formation events. *Atmos. Chem. Phys.* **10**: 7907–7927, doi: 10.5194/acp-10.7907-2010.

Merikanto J, Napari I, Vehkamäki H, Anttila T, Kulmala M. 2007. New parameterization of sulfuric acid–ammonia–water ternary nucleation rate at tropospheric conditions. *J. Geophys. Res.* **112**(,): D15207, doi: 10.1029/2006JD007977.

Metzger A, Verheggen B, Dommen J, Duplissy J, Prevot ASH, Weingartner E, Riipinen I, Kulmala M, Spracklen DV, Carslaw KS, Baltensperger U. 2010. Evidence for the role of organics in aerosol particle formation under atmospheric conditions. *Proc. Natl. Acad. Sci. U.S.A.* **107**: 6646–6651.

Mirme S, Mirme A. 2013. The mathematical principles and design of the NAIS – a spectrometer for the measurement of cluster ion and nanometer aerosol size distributions. *Atmos. Meas. Tech.* **6**: 1061–1071.

Modgil MS, Kumar S, Tripathi SN, Lovejoy ER. 2005. A parameterization of ion-induced nucleation of sulphuric acid and water for atmospheric conditions. *J. Geophys. Res.* **110**: D19205, doi: 10.1029/2004JD005475.

Mönkkönen P, Koponen IK, Lehtinen KEJ, Hämeri K, Uma R, Kulmala M. 2005. Measurements in a highly polluted Asian mega city: Observations of aerosol number size distribution, modal parameters and nucleation events. *Atmos. Chem. Phys.* **5**: 57–66.

Nadykto AB, Yu F. 2003. Uptake of neutral polar vapor molecules by charged clusters/particles: enhancement due to dipole–charge interaction. *J. Geophys. Res.* **108**: 4717, doi: 10.1029/2003JD003664.

Neitola K, Asmi E, Komppula M, Hyvarinen A-P, Raatikainen T, Panwar TS, Sharma VP, Lihavainen H. 2011. New particle formation infrequently observed in Himalayan foothills – why? *Atmos. Chem. Phys.* **11**: 8447–8458.

O'Dowd CD, Aalto P, Hmeri K, Kulmala M, Hoffmann T. 2002. Aerosol formation: atmospheric particles from organic vapours. *Nature* **416**: 497–498.

Ortega IK, Suni T, Boy M, Grönholm T, Manninen HE, Nieminen T, Ehn M, Junninen H, Hakola H, Hellén H, Valmari T, Arvela H, Zegelin S, Hughes D, Kitchen M, Cleugh H, Worsnop DR, Kulmala M, Kerminen V-M. 2012. New insights into nocturnal nucleation. *Atmos. Chem. Phys.* **12**: 4297–4312.

Porstendörfer J. 1994. Properties and behaviour of radon and thoron and their decay products in the air. *J. Aerosol Sci.* **25**: 219–263.

Prasad BSN, Nagaraja K, Chandrashekara MS, Paramesh L, Madhava MS. 2005. Diurnal and seasonal variation of radioactive and electrical conductivity near the surface for a continental location Mysore, India. *Atmos. Res.* **76**: 65–77.

Ranalkar MR, Mishra RP, Anjan A, Krishnaiah S. 2012. Network of automatic weather stations: Pseudo random burst sequence type. *Mausam* **63**: 587–606.

Rawal A, Tripathi SN, Michael M, Srivastava AK, Harrison RG. 2013. Quantifying the importance of galactic cosmic rays in cloud microphysical processes. *J. Atmos. Sol.-Terr. Phys.* **102**: 243–251, doi: 10.1016/j.jastp.2013.05.017.

Reischl GP, Mäkelä JM, Karch R, Necid J. 1996. Bipolar charging of ultrafine particles in the size range below 10 nm. *J. Aerosol Sci.* **27**: 931–949.

Shi Q, Sakurai H, McMurry PH. 2007. Characteristics of regional nucleation events in urban East St Louis. *Atmos. Environ.* **41**: 4119–4127, doi: 10.1016/j.atmosenv.2007.01.011.

Siingh D, Singh RP. 2010. The role of cosmic rays on the Earth's atmospheric processes. *Pramana-J. Phys.* **74**: 153–168.

Siingh D, Pant V, Kamra AK. 2011. The ion–aerosol interaction from the ion mobility and aerosol particle size distribution measurements on January 17 and February 18 2005 at Maitri, Antarctica – a case study. *J. Earth Syst. Sci.* **120**: 735–754.

Siingh D, Gautam AS, Kamra AK, Komsaare K. 2013. Nucleation events for the formation of charged aerosol particles at a tropical station – preliminary results. *Atmos. Res.* **132–133**: 239–252, doi: 10.1016/j.atmosres.2013.05.024.

Stanier CO, Kylstov AY, Pandis SN. 2004. Nucleation events during the Pittsburgh air quality study: description and relation to key meteorological, gas phase, and aerosol parameters. *Aerosol Sci. Technol.* **38**: 253–264.

Stolzenburg MR, McMurry PH, Sakurai H, Smith JN, Mauldin RL III, Eisele FL, Clement CF. 2005. Growth rates of freshly nucleated atmospheric particles in Atlanta. *J. Geophys. Res.* **110**: D22S05, doi: 10.1029/2005JD005935.

Tammet H. 1995. Size and mobility of nanometer particles, clusters and ions. *J. Aerosol Sci.* **26**: 459–475.

Tammet H, Komsaare K, Hõrrak U. 2013. Estimating neutral nanoparticle steady-state size distribution and growth according to measurements of intermediate air ions. *Atmos. Chem. Phys.* **13**: 9597–9603.

Tinsley BA, Rohrbaugh RP, Hei M, Beard K. 2000. Effects of image charges on scavenging of aerosol particles by cloud droplets and on droplet charging and possible ice nucleation processes. *J. Atmos. Sci.* **57**: 2118–2134.

Tripathi SN, Harrison RG. 2001. Scavenging of radioactive aerosol. *Atmos. Environ.* **35**: 5817–5821.

Tripathi SN, Harrison RG. 2002. Enhancement of contact nucleation by scavenging of charged aerosol particles. *Atmos. Res.* **62**: 57–70.

Tunved P, Hansson H-C, Kerminen V-M, Ström J, Dal Maso M, Lihavainen H, Viisanen Y, Aalto PP, Komppula M, Kulmala M. 2006. High natural aerosol loading over boreal forests. *Science* **312**: 261–263.

Vana M, Ehn M, Petäjä T, Vuollekoski H, Aalto P, de Leeuw G, Ceburnis D, O'Dowd CD, Kulmala M. 2008. Characteristic features of air ions at Mace Head on the west coast of Ireland. *Atmos. Res.* **90**: 278–286.

Vartiainen E, Kulmala M, Ehn M, Hirsikko A, Junninen H, Petäjä T, Sogacheva L, Kuokka S, Hillamo R, Skorokhod A, Belikov I, Elansky N, Kerminen V-M. 2007. Ion and particle number concentrations and size distributions along the Trans-Siberian railroad. *Boreal Environ. Res.* **12**: 375–396.

Venzac H, Sellegri K, Laj P. 2007. Nucleation events detected at the high altitude site of the Puy de Dôme Research Station, France. *Boreal Environ. Res.* **12**: 345–359.

Venzac H, Sellegri K, Laj P, Villani P, Bonasoni P, Marinoni A, Cristofanelli P, Calzolari F, Fuzzi S, Decesari S, Facchini M-C, Vuillermoz E, Verza GP. 2008. High frequency new particle formation in the Himalyas. *Proc. Natl. Acad. Sci. U.S.A.* **105**: 15666–15671.

Vohra KG, Subba Ramu MC, Muraleedharan TS. 1984. An experimental study of the role of radon and its daughters in the conversion of sulphur dioxide into aerosol particles in the atmosphere. *Atmos. Environ.* **18**: 1653–1656.

Weber RJ, Marti JJ, McMurry PH, Eisele FL, Tanner DL, Jefferson A. 1997. Measurements of new particle formation and ultrafine particle growth rates at a clean continental site. *J. Geophys. Res.* **102**: 4375–4385, doi: 10.1029/96JD03656.

Yli-Juuti T, Riipinen I, Aalto PP, Nieminen T, Maenhaut W, Janssens IA, Claeys M, Salma I, Ocskay R, Hoffer A, Imre K, Kulmala M. 2009. Characteristics of new particle formation events and cluster ions at K-puszta, Hungary. *Boreal Environ. Res.* **14**: 683–698.

Yli-Juuti T, Nieminen T, Hirsikko A, Aalto PP, Asmi E, Hõrrak U, Manninen HE, Patokoski J, Dal Maso M, Petäjä T, Rinne J, Kulmala M, Riipinen I. 2011. Growth rates of nucleation mode particles in Hyytiälä during 2003–2009: variation with particle size, season, data analysis method and ambient conditions. *Atmos. Chem. Phys.* **11**: 12865–12886, doi: 10.5194/acp-11-12865-2011.

Yu FQ. 2001. Chemiions and nanoparticle formation in diesel engine exhaust. *Geophys. Res. Lett.* **28**: 4191–4194, doi: 10.1029/2001GL013732.

Yu, F. 2003. Nucleation rate of particles in the lower atmosphere: Estimated time needed to reach pseudo-steady state and sensitivity to H_2SO_4 gas concentration. *Geophys. Res. Lett.* **30**: 1526, doi: 10.1029/2003GL017084.

Yu FQ. 2010. Ion-mediated nucleation in the atmosphere: key controlling parameters, implications, and look-up table. *J. Geophys. Res.* **115**: D03206, doi: 10.1029/2009JD012630.

Yu FQ, Turco RP. 2000. Ultrafine aerosol formation via ion-mediated nucleation. *Geophys. Res. Lett.* **27**: 883–886, doi: 10.1029/1999GL011151.

Yu FQ, Turco RP. 2001. From molecular clusters to nanoparticles: role of ambient ionization in tropospheric aerosol formation. *J. Geophys. Res.* **106**: 4797–4814, doi: 10.1029/2000JD900539.

Yu FQ, Turco RP. 2011. The size-dependent charge fraction of sub-3-nm particles as a key diagnostic of competitive nucleation mechanisms under atmospheric conditions. *Atmos. Chem. Phys.* **11**: 9451–9463.

Yu FQ, Wang Z, Luo G, Turco RP. 2008. Ion-mediated nucleation as an important global source of tropospheric aerosols. *Atmos. Chem. Phys.* **8**: 2537–2554.

Yu FQ, Luo G, Bates T, Anderson B, Clarke A, Kapustin V, Yantosca R, Wang Y, Wu S. 2010. Spatial distributions of particle number concentrations in the global troposphere: simulations, observations, and implications for nucleation mechanisms. *J. Geophys. Res.* **115**: D17205, doi: 10.1029/2009JD013473.

Yue DL, Hu M, Wu Z, Wang Z, Guo S, Wehner B, Nowak A, Achtert P, Wiedensohler A, Jung J, Kim YJ, Liu S. 2009. Characteristics of aerosol size distributions and new particle formation in the summer in Beijing. *J. Geophys. Res.* **114**: D00G12, doi: 10.1029/2008JD010894.

Zhang RY, Suh I, Zhao J, Zhang D, Fortner EC, Tie X, Mo Molina LT, Molina MJ. 2004. Atmospheric new particle formation enhanced by organic acids. *Science* **304**: 1487–1490.

